SYNTHESIS, CHARACTERIZATIONS AND PHOTOVOLTAIC APPLICATIONS OF DITHIENOTHIOPHENE AND BENZOTRIAZOLE CONTAINING CONJUGATED POLYMERS

A THESIS SUBMITTED TO
THE GRADUATE SCHOOL OF NATURAL AND APPLIED SCIENCES
OF
MIDDLE EAST TECHNICAL UNIVERSITY

BY

ŞEVKİ CAN CEVHER

IN PARTIAL FULFILLMENT OF THE REQUIREMENTS
FOR
THE DEGREE OF MASTER OF SCIENCE
IN
CHEMISTRY

SEPTEMBER 2013

Approval of the thesis:

SYNTHESIS, CHARACTERIZATIONS AND PHOTOVOLTAIC APPLICATIONS OF DITHIENOTHIOPHENE AND BENZOTRIAZOLE CONTAINING CONJUGATED POLYMERS

submitted by **ŞEVKİ CAN CEVHER** in partial fulfillment of the requirements for thedegree of **Master of Science in Chemistry Department, Middle East TechnicalUniversity** by,

Prof. Dr. Canan Özgen
Dean, Graduate School of **Natural and Applied Sciences** _____

Prof. Dr. İlker Özkan
Head of Department, **Chemistry** _____

Assoc. Prof. Dr. Ali Çırpan
Supervisor, **Chemistry Dept., METU** _____

Prof. Dr. Levent Toppare
Coadvisor, **Chemistry Dept., METU** _____

Examining Committee Members:

Assoc. Prof. Dr. Tamer Uyar
Inst. of Mat. Sci. & NanotechnologyUNAM/Bilkent _____

Assoc. Prof. Dr. Ali Çırpan
Chemistry Dept., METU _____

Prof. Dr. Levent Toppare
Chemistry Dept., METU _____

Assist. Prof. Dr. İrem Erel
Chemistry Dept., METU _____

Assist. Prof. Dr.Akın Akdağ
Chemistry Dept., METU _____

Date:04.09.2013

I hereby declare that all information in this document has been obtained and presented in accordance with academic rules and ethical conduct. I also declare that, as required by these rules and conduct, I have fully cited and referenced all material and results that are not original to this work.

Name, Last name: **ŞEVKİ CAN CEVHER**

Signature:

ABSTRACT

SYNTHESIS, CHARACTERIZATIONS AND PHOTOVOLTAIC APPLICATIONS OF DITHIENOTHIOPHENE AND BENZOTRIAZOLE CONTAINING CONJUGATED POLYMERS

Cevher, Şevki Can

M.Sc., Department of Chemistry

Supervisor: Assoc. Prof. Dr. Ali Çırpan

Coadvisor: Prof. Dr. Levent Toppare

September 2013, 53 pages

Fused bithiophene containing conjugated polymers are recently used in different applications; for example organic light emitting diodes, solar cells, electrochromic devices and organic field effect transistors. Fused bithiophene derivatives increase the planarity, charge mobility and decrease band gap when incorporated into the polymer backbone. Connecting atom between the bithiopheneunit can be phosphorous, silicon, nitrogen and sulphur. In this thesis, dihienothiophene was coupled with benzotriazole via Stille Coupling and synthesized polymers were used in optoelectronic applications. Molecular weight and thermal behavior were investigated with GPC, TGA and DSC analysis. Oxidation and reduction behaviors of the polymers were studied with cyclic voltammetry. The absorption properties of the conjugated polymers in solution and film were investigated. After optimizing thickness and morphologies of polymer:PCBM, device production and current/voltage property measurements were conducted in a nitrogen-filled glovebox system (moisture <0.1 ppm; oxygen <0.1 ppm). The analysis of the photovoltaic devices (ITO/PEDOT:PSS/polymer:PCBM/Metal) was performed by means of the energy conversion efficiency measured under standard AM1.5 G illumination (100mW.cm^{-2}).

Keywords: benzotriazole, conjugated polymers, dithienothiophene, electrochemistry, electrochromism, organic solar cell, synthesis.

ÖZ

DİTİYENOTİYOFEN VE BENZOTRİAZOL İÇEREN KONJÜGE POLİMERLERİN SENTEZİ, KARAKTERİZASYONU VE FOTOVOLTAYİK UYGULAMALARI

Cevher, Şevki Can

Yüksek Lisans, Kimya Bölümü

Tez yöneticisi: Doç. Dr. Ali Çırpan

Tez yardımcı yöneticisi: Prof. Dr. Levent Toppare

Eylül 2013, 53 sayfa

Bitişik tiyofenleri içeren konjüge polimerler son zamanlarda organic güneş pillerinde, ışık saçan diyotlarda, elektrokromik malzemelerde ve organik transistörlerde kullanılmaktadır. Bitiyofen türevleri eklendikleri polimerlerin düzlemselliğini ve konjügasyonunu arttırmakta ve bant aralığını düşürmektedir. Bitiyofen arasındaki atom fosfor, silikon, azot ve kükürt olabilmektedir. Bu tezde ditiyenotiyofen benzotriazol ile Stille kenetlenme reaksiyonu ile sentezlendi ve sentezlenen polimerler optoelektronik uygulamalarda kullanıldı. Molekül ağırlığı ve ısısal davranışları GPC, TGA ve DSC ile keşfedildi. İndirgenme ve yükseltgenme davranışları Dönüşümlü Voltametri ile çalışıldı. Spektroskopik teknikler kullanılarak yapısal analizlerine bakıldı ve çözeltide ve filmdeki polimerlerin ışığı soğurma özellikleri incelendi. Son olarak kalınlığın ve morfolojinin optimizasyonu yapıldıktan sonra, pilin üretimi ve akım/gerilim özelikleri azot dolu eldivenli kabin sisteminde gerçekleştirildi (nem< 0,1 nm; oksijen< 0,1 ppm). Güneş pillerinin (ITO/PEDOT: PSS/polimer:PCBM/ metal) analizleri güç çevirim verimi AM 1,5 Gaydınlatma ile hesaplandı (100 $mW.cm^{-2}$).

Anahtar kelimeler: benzotriazole, kojugepolimerler, ditiyanotiyofen, elektrokimya, elektrokromizm, organic güneş pili, sentez.

To INDESTRUCTIBLE THOUGHTS

ACKNOWLEDGEMENTS

First and foremost, I am grateful to my supervisor Assoc. Prof. Dr. Ali Çırpan for his eternal patience, expertise, endless care and opportunities that are given me to do this work.

I would like to thank my co-advisor Prof. Dr. Levent Toppare, for his support and valuable suggestions.

Words are intimately meaningless to express my feelings, pleasure and gratefulness to their friendship, Buket Zaifoğlu and Ali Can Özelçağlayan. I owe for their support in any circumstances.

Special thanks to Bengisu Çorakçı for her help and mostly for fun journeys with her.

Thanks for good friendship, Metin Karayılan, Şebnem Bayseç, SimenToksabay, Seza Göker.

I would like to thank to Ezgi Demircan, Seda Okumus, Duygu İşibol, Serkan Eymur, Eylem Canbolat, Melek Parlak, as a whole all ASD research group, for their support and some interesting advices.

Thanks go to Naime Akbaşoğlu Ünlü, Yasemin Udum, Doğukan Hazar Apaydın for their help in this study.

Thanks for sharing fun time, Erdem Seçkin, Haluk Ziya Erçek, Bulut Barış Altun, Muhammet Küçüktiftik, Duygu Yılmaz, Oğuz Kaan Öztürk, Umut Canlı.

I would like to express my gratitude to Prof. Dr. Halil İbrahim Ünal for everything.

Thanks for everthing, all Toppare and Çırpan research group members.

Finally, for their patience, support, and inspiration I would like to represent my pleasure to my family.

TABLE OF COTENTS

LIST OF TABLES

LIST OF SCHEMES

LIST OF FIGURES

LIST OF ABBREVIATIONS

PCE	Power conversion efficiency
OSC	Organic solar cell
HOMO	Highest occupied molecular orbital
LUMO	Lowest unoccupied molecular orbital
SLC	Single layer cell
DLC	Double layer cell
BHJ	Bulk heterojunctioncell
LC	Laminated cell
ITO	Indium tin oxide
PEDOT	Polyethylenedioxythiophene
PSS	Polystyrenesulfonate
PCBM	[6,6]-Phenyl C_{61} butyric acid methyl ester
EA	Electron affinity
IP	Ionization potential
Wf	Work function
V_{oc}	Open circuit voltage
EQE	External quantum efficiency
JV	Current density-voltage
J_{sc}	Short circuit current density
FF	Fill factor
P_{max}	Maximum power
R_l	Load resistor
R_{sh}	Shuntr esistor
R_s	Series resistor
η	Power conversion efficiency

P_{inc}	Power of the incident light
AM 1.5G	Air mass 1.5 global
R	Reducing agent
O	Oxidizing agent
E_g	Band gap
DA	Donor-acceptor
BTz	Benzotriazole
OFET	Organic field effect transistors
DTT	Dithienothiophene
UV	Ultraviolet
Vis	Visible
CV	Cyclic voltammetry
GPC	Gel Permeation chromatography
THF	Tetrahydrofuran
TGA	Thermal gravimetric analysis
$TBAPF_6$	Tetrabutylammoniumhexafluorophosphate
ACN	Acetonitrile
NHE	Normal hydrogen electrode
E_g^{opt}	Optic band gap
E_g^{el}	Electronic band gap
NIR	Near infrared
CIE	International Commission on Illumination
L	Luminance
a	Hue
b	Saturation
IPCE	Incident photon to current efficiency

CHAPTER 1

INTRODUCTION

1.1 General Introduction

There is no more attractive method for obtaining energy to convert it than to harvest directly from sun. Earth receives 1.75x 10^{17} W energy from sun. Total energy consumption of whole world was 4.4x 10^{20} J in 2003. Although the total conversion of energy is not possible it still remains great importance. State-of-the-art inorganic solar cells readily reached to power conversion efficiency (PCE) of 39% [1]. However, commercial ones reach 15-20%. On the other hand, PCEs of the less effective-due to be less investigated-counterpart organic solar cells (OSC) reach up only 12% by a private agency [2]. Efficiency of solar cellconstructed with organic semiconductors is limited, however they have unique attractions to investigate and all of these will partially be emphasized on upcoming sections.

1.2 Organic Semiconductors

It is often difficult to compare organic and inorganic semiconductors. Due to strong interaction of electron-phonon of the former ones, they could not be classified in the same manner. Moreover, there are various blind spots that scientist needed to be enlightened about various differences of organic semiconductors.

Among them, the most obvious difference is binding energy. Photo-excitation does not directly lead to formation of free charge carriers in contrast to inorganic semiconductors. Yet bounded electron-hole (exciton) pair is formed and the energy needed to separate this pair is about 0.4 eV which is called as binding energy.[3-5]

Semiconductivity is described by band theory for highly ordered inorganic crystalline materials. In highly ordered inorganic semiconductors there are conduction bands and valence bands. Hence conductance is established via introducing electron through a conduction band. However in organic polymeric semiconductors, there is no definite lattice in solid state and band theory is insufficient to describe the conductance in organic polymeric materials. Hence conductance can be described by delocalization of electrons through a way of conjugation, thanks to the molecular orbital theory and hybrid orbital theory. Hybridization of carbon atoms in conjugation pathway is generally sp^2 hybridized. Carbon atoms are bonded linear or in an aromatic system with another carbon with one of this sp^2 hybridized and one additional unhybridized off-axis $p_z$orbital,

in order to maintain conjugation. Molecular orbital theory enables us to draw discrete energy levels of electrons in this system. Although the energy gap between valence band and conductance band described in inorganic materials, there is no valence or conductance band for polymeric material. Instead the energy gap is defined as the energy levels splitting between the bonding and antibonding orbitals formed in between p_z orbitals of neighboring carbons. HOMO (Highest Occupied Molecular Orbital) and LUMO (Lowest Unoccupied Molecular Orbital) take stage at this point and become analogous, in inorganic semiconductors, top of the valence band and bottom of conductance band. Then energy gap is the energy differences between HOMO and LUMO and the magnitude of it is inversely proportion to the conjugation length. If the delocalization segments are adjusted particle in a box system, according to the quantum mechanics, energy gap between levels are getting smaller and smaller when the length of conjugation is increased.

1.3 Low Band Gap Polymers

Magnitude of band gaps of polymers in various applications is directly related with the aim. For these applications, luckily, the needed band gaps are as small as the semiconductors have. In electrochromic applications, color must be changed upon applied potential and color is a wave of light what human eyes see. Generally, materials used in electrochromic devices have absorption bands in between 400 nm and 700 nm in order to maintain proper color change. If color is intended to be converted to its responsible energy than it is simply between 3 eV and 1.8 eV respectively according to the formula:

$E = \frac{\mathrm{h\ x\ c}}{\lambda}$and if units are converted properly;$E = \frac{1240\ \mathrm{eV/nm}}{\lambda}$ Equation 1.1

It is also valid for light emitting diodes. Diodes used in displays or somewhere else should have proper band gaps to emit colored light. Moreover in photovoltaic applications, absorption bands of materials should be well overlapped with solar spectrum. It should be clearly stated that irradiation of sun reaches to earth surface is in mainly visible and has great extend to infrared regions. In order to convert the sun light into electricity photovoltaic device must absorb incoming light. How much a material absorbs light is directly related with constructed device efficiency. Low band gap polymers are great candidates for broad solar spectrum absorption and also highly efficient photovoltaic devices [6].

There are various ways of to obtain low band gap polymers. These are mainly,decreasing bond length alternation, donor-acceptor type synthesis, increasing π-conjugation length and controlling the steric interaction between adjacent units not to disturb co-planarity[7]

Quinoid structure of polythiophene is slightly effective in its ground state. Hence the linkage between two thiophenes has mainly single bond characteristics, a large bond length alternation is observed. In order to increase its double bond behavior,

energetically more favorable quinoid like structure can be manipulated [8]. As in the case of polyisothianapthene, favorable quinoid structure enhances the double bond characteristic of the linkage between two adjacent thiophenes. There is a tendency to decrease the band gap in which conjugated polymers inducing quinoid form in their ground states.

In the concept of donor-acceptor [9], conjugated polymer chain consisting of a donor with high lying HOMO and an acceptor with low lying LUMO leads narrow band gap and wide band with [10,11]. Although wide band width is essential for high mobility and low band gap is necessary for intrinsic conductivity, it is not always applicable for all systems. If there is weak interaction between donor and acceptor units then there is no problem to obtain small band gap. However, band width gets smaller. On the other hand, if there is strong interaction in between the two units band gap increases due to strong charge transfer. In **Figure 1.1** it is schematically illustrated having high band gap and small band width. Moreover it should be emphasized that conductivity of homopolymers is higher than that of the donor-acceptor types. Although the conductivity is increased via doping the homopolymerswith Iodine vapor by 15 times, in donor-acceptor type conjugated polymer it is increased just 2 or 3 orders of magnitude [12].

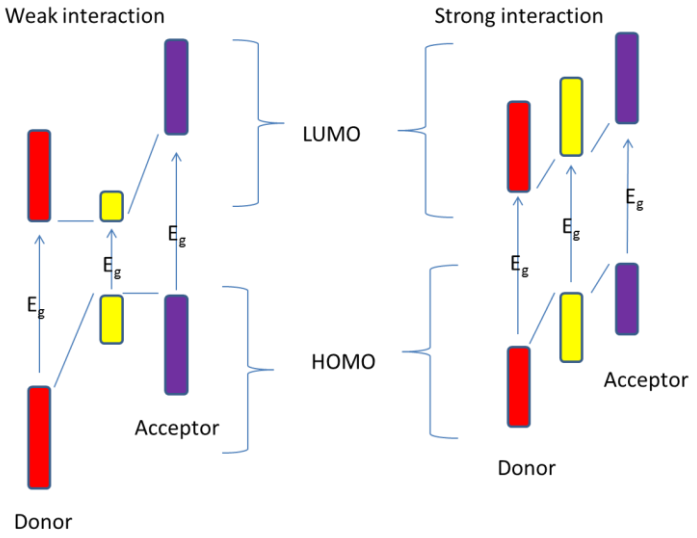

Figure 1.1 Interactions in Donor-Acceptor

Actually band gap (E_g) is altered according to the equation 1.2[13]:

$$E_g = E^{\delta r} + E^{\theta} + E^{res.} + E^{sub.} + E^{int.}$$ Equation 1.2

$E^{\delta r}$: bond length alternation along the chain

E^{θ}: mean deviation from planarity

$E^{res.}$: aromatic resonance energy of the ring

$E^{sub.}$: inductive or mesomeric electronic effects of substitutients

$E^{int.}$: inter-chain or intermolecular coupling in the solid state.

1.4 Organic Solar Cells

In order to convert sunlight into electricity using organic materials, tremendous investigation has been done within the last three decades [14-22]. Due to poor charge carrier mobility of organic semiconductors [23] the design and efficiency of organic solar cells possess various differences compared to inorganics. Hence their mobilities are low it can be compensated by generally high absorptivity of organic materials. Thus devices prepared with thin organic layers can be efficient to effectively absorb light. Moreover, as a hole conductor most of organic semiconductors have around 2 eV band gap which limits the harvesting of solar spectrum. Hence solubility can be introduced by structural modifications of organic materials; band gap can also be tuned via this method. However exciton diffusion length in organic materials is very limited due to binding energy. Before exciton recombines it must be dissociated into free charge carriers, main elements of solar cells. To establish efficient dissociation diffusion length should not be more than 20 nm [24].These features of organic materials lead us to construct light weight, flexible and thin organic solar cells. A device constructed in our laboratory on a glass substrate is shown in below **Figure 1.2** and it can be predicted how light the device is. Extra weight on a glass substrate is almost 10 mg.

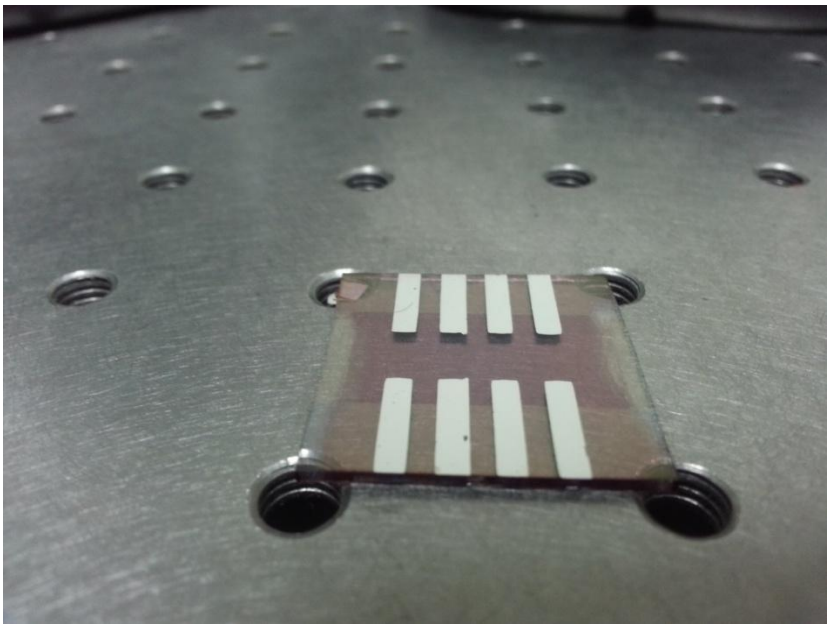

Figure 1.2 A solar cell device

1.4.1 Types of Organic Solar Cells

There are various types of solar cells in the literature. Single layer cells (SLC) are composed of only one semiconductor material in between two electrodes. In this type of devices one electrode is Schottky (rectifying) in which the charge separation occurs, the other electrode is ohmic. In SLCs full visible absorption is rare and due to thin photoactive layer absorption of light is insufficient. Moreover, after separation of exciton into free charges, these travel through the same layer therefore risk of recombination is ultimate. Double layer cells (DLC)are composed of two different layers. After exciton dissociation separated charges travel through different materials and recombination is minimized. However, small interface area, where charge separation is achieved, is drawback of DLCs. Bulk heterojunction cells (BHJ) have excellent charge separation interface if good molecular mixing is achieved. The defect is the partial connectivity of correct electrode and the network structure. Laminated cells (LC) benefit the combination of BHJ and DLC. Charge separation is well established after laminating two different layers together and separated charges are transported to correct electrodes. However advanced techniques and devices must be accompanied. Also low glass transition temperature is the main importance when organic semiconductors form the intermixed layer.

1.4.1 Organic Bulk Heterojunction Solar Cells Device Structure

In **Figure 1.3** the general bulk-heterojunction type organic solar cell, which was used in this study, is shown. Indium tin oxide (ITO) coated glass substrate is used as the anode and aluminum metal is used as the cathode. Between anode and cathode active layer is inserted. Solution of donor and acceptor blend is coated onto PEDOT (polyethylenedioxythiophene): PSS (polystyrenesulfonate) coated ITO substrate via various techniques such as spin coating. There can be various layers such as calcium, lithium fluoride and so on before external electrode is deposited. External electrode is generally used to protect the inner electrodes which are sensitive to oxygen and can easily get oxidized.

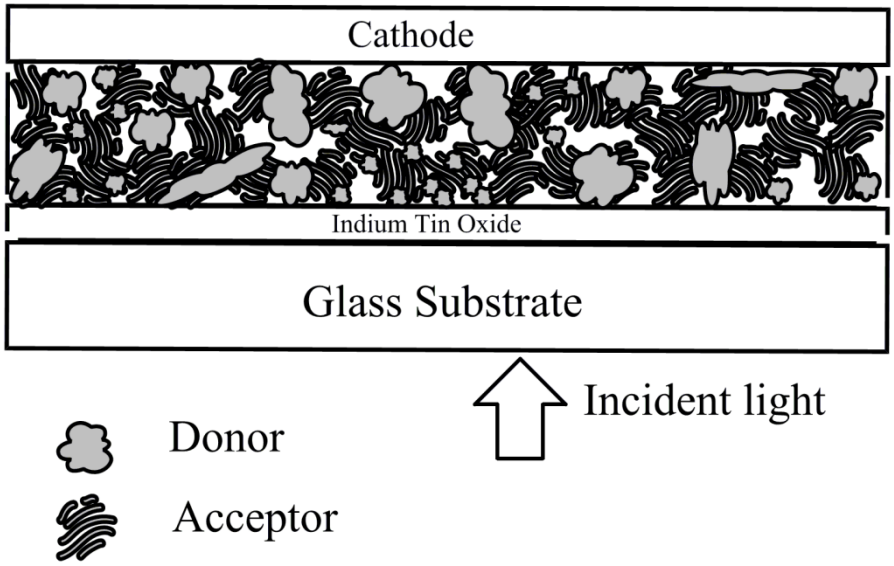

Figure 1.3 Bulk-Heterojunction solar cell device structure

1.4.2 Operation Principle of Organic Solar Cells

As a device, solar cell converts light into electricity. Using ITO coated glass substrate as anode is simply requirement of a transmissive electrode to allow light pass through to active layer. Firstly, absorption of light in the active layer starts the conversion. At this time, donor represents organic semiconductor materials and acceptor represents generally used PCBM ([6,6]-Phenyl C_{61} butyric acid methyl ester).Absorption of light leads to photoexcitations in donor species. As an electron in HOMO of the donor is excited to LUMO, there will be extra electron in LUMO and there will be an absence of electron in HOMO. Then columbic attraction between HOMO (positive hole due to absence of electron) and LUMO (negative charge due to extra electron) takes place. In order to separate this hole-electron pair (exciton) as a free charge, exaction must travel to donor-acceptor interface. However the distance that exciton can travel is restricted. Before exciton recombine- relaxation of electron in LUMO back to HOMO- exciton must reach to donor-acceptor interface. At donor-acceptor interface there must be a driving force to push forward each of charges through to different electrodes. This can be established in the case of the differences between LUMO levels of donor and acceptor is bigger than the binding energy. After successful dissociation of exciton, holes will be collected at anode and electrons will be collected at cathode. Introducing external circuit electricity can be obtained. In **Figure 1.4** energy conversion will schematically be described.

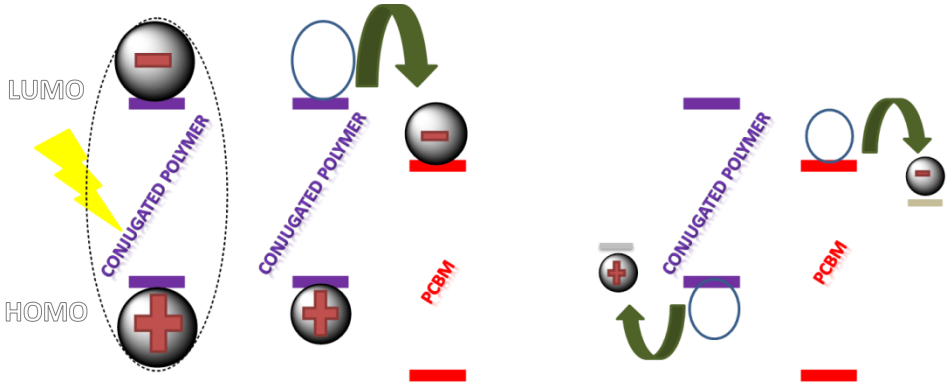

Figure 1.4 Energy conversion in bulk-heterojuncton solar cells where donor is chosen as conjugated polymer and acceptor asPCBM (Phenyl-C61-butyric acid methyl ester) which is commercially available.

Although the objective is converting sun light into electricity, great extent of photon comes from sun is lost due to following reasons. Firstly, reflected and transmitted light cause less exciton formation. Recombination of excitons and free charges are also other mechanisms of losing energy. Thus less efficient performances are observed.

1.4.2.1 Donor/Acceptor Interface

In order to construct an efficient solar cell, one should be careful about the donor/acceptor interface where the free charge separation occurs. If one material with higher electron affinity (EA) and one material with lower ionization potential (IP) are blended to form active layer of bulk heterojunction solar cell, as it is seen in the figure required transfer of charges might be collected. As accepting an electron to a LUMO of acceptor whose EA is greater and accepting a hole from the HOMO of the contacting material whose IP is lower. The important thing that should be emphasized for organic semiconductors offset of IP and EA should be large enough to overcome the exciton binding energy, typically 0.4 eV. If this cannot be satisfied charge transfer might be achieved but exciton does not split into free charges and ultimately they recombine at donor/acceptor interface. Thus absorbed sun light is lost and efficiency got decreased. Also exciton can transfer its energy if both the hole and electron decreases their energy as it is seen in the figure. This kind of transfer, with some energy loss, is known as Foerster energy transfer. This allows us to design possibly a one way directionality of exciton diffusion from higher bandgap to lower band gap material.

1.4.2.2 Electrode/Semiconductor Interface

In 1938, Mott and Schottky explained the concept of contacts between metal and doped semiconductor [25,26]. Although the charge injection from metallic conducts into inorganic semiconductor is not exactly same with that of the organic semiconductors, in this thesis basics of the latter one will be mentioned.

Charge injection can be simply divided into two main categories, before contact and after contact. After contact bending occurs in the direction which depends on whether the work functions (W_f) of the contacting electrodes are below or above the Fermi level of the semiconductors. Upon contact, Fermi levels of semiconductors tend to equalize. For practical use, Fermi level can be assumed to lie around the middle of the bandgap. Also qualitatively predicted bendings are shown in the figure where they can be seen blocking and nonblocking type bendings. Bending depends on position of the Fermi level, and n-type or p-type semiconductors can be classified relative position to LUMO or HOMO respectively. Hence, under equilibrium condition- dark and no applied voltage-balance between the concentration of occupations holes and electrons simply represents the Fermi level. If work functions of electrodes are deeper inside the band gap than the Fermi levels of contacting semiconductors, bending occurs such a way that seen in fig a before photoexcited electrons reach to Al electrode from LUMO of acceptor, they encounter a barrier due to blocking contact. Similar analog is also true for holes from HOMO of the donor to ITO. Thus current is decreased. Hence upon changing the potential of these electrodes contacts play the role of non-blocking character and they are called as rectifying or Schotky contacts.

Au and Ca electrodes give higher open circuit voltage (V_{oc}) and higher current instead of a device using ITO and Al and also higher external quantum efficiency (EQE).[27,28]Lower W_f of Ca, it is more prone to oxidation and Au electrode is expensive and hard to process. Devices fabricated with Al and ITO are inexpensive and easilyreproducible. These features make help to ignore the negative effects of blocking contacts.

1.4.3Structuralproperties of Organic Semiconductors Used in Bulk Heterojunction Solar Cells

Beside their curial optical and electronic properties, organic semiconductors should have vital mechanical properties to be used in BHJs. Via thermal sublimation high vacuum and high temperature are required and at these circumstances semiconductor material should be stable. However, the technique used in this thesis; processing from solution simply by spin coating can be done at atmospheric pressure and room temperature. Organic semiconductors can be categorized due to their mechanical and processing properties. Monomers (single unit) and oligomers (a few repeating unit) that absorb visible sunlight are generally called as chromophores. If they are soluble then they are

referred to as dyes if not then they are referred to as pigments. Liquid crystalline material at certain temperature exhibits a phase moves like in a liquid and still sustains a certain structural order. Different types of liquid crystalline materials are found in the literature but here detailed explanation will not be given. **Figure 1.5** clearly shows the structural differences. The mechanical properties processability and π-π stacking and so on mainly depends on the position, properties and number of the side chains. Constituent of the main chain is mainly related with the optic and electronic properties. Side chains are generally attached to molecules that lack of solubility to improve. Due to strong π-π interaction flat molecules have a great tendency to aggregate or stick together in solution. Bulky side chain makes them separate to be surrounded by solvent molecules individually and the situation which is called as dissolution. Naturally small molecules are better soluble but larger molecules have better film morphology upon spin coating. Polymers are excellent candidates to be used as semiconductor as easily mechanically modified materials.

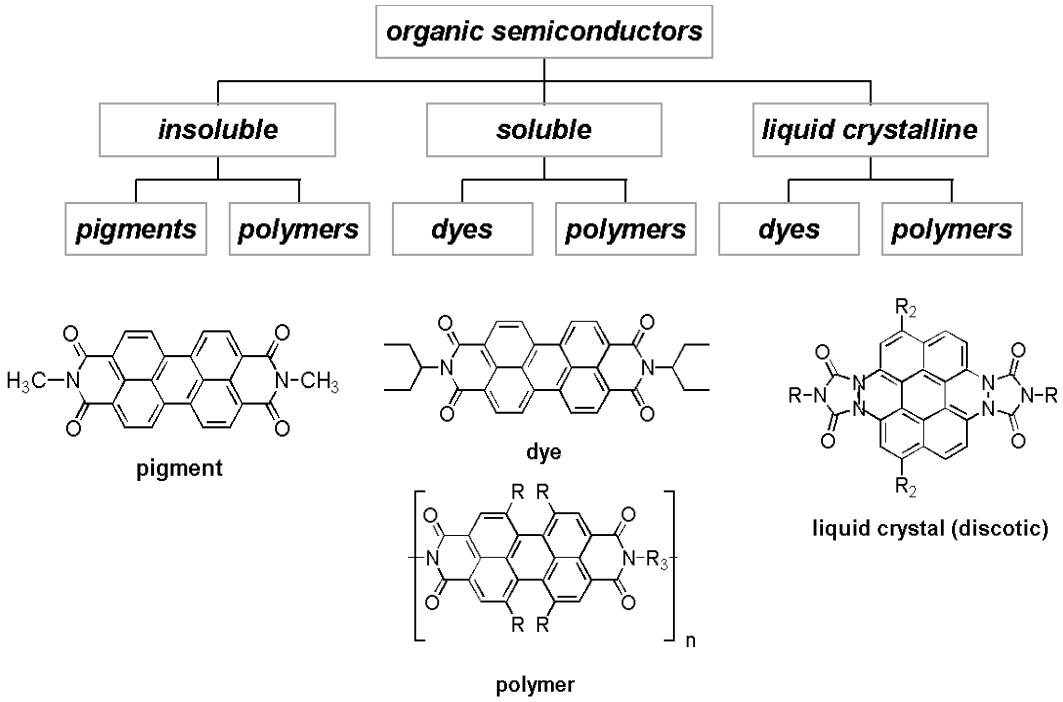

Figure 1.5 Structural differences of organic molecules

1.4.4Photovoltaic Properties

Practically, relaxation of photoexcited electrons to lowest lying level of LUMO is fast and called as thermalization since heat is dissipated. As a result of this process bandgap

can be supposed to be a measure for achievable voltage. However, synthesis of low band gap materials is ultimate purpose to harvest maximum portion of solar light. Although the aim is low band gap there is a limitation which was described by Shockley and Queisser [29]. Only radiative recombination and under the solar radiation of earth, semiconductor as silicon should have a band gap of 1.12 eV to achieve 30% power conversion efficiency [30].

Since the higher the resistor the lower the current and the more time for charges to get out of semiconductor, recombination is inevitably being dominant. This characteristic can be seen in current density-voltage (*J*V) graph in **Figure1.6**. According to the graph maximum power that can be obtained from a device can be found in the fourth quadrant. The point (J_{max}, V_{max}) where multiplicity of *J* and V gets its higher value is the maximum power that can be obtained. If the shape of curve gets more rectangular power gets increased. Thus the ratio of J_{sc}(short circuit current density) xV_{oc}(open circuit voltage) and J_{max}xV_{max}quality of the curve, which is namely fill factor (FF).

$$FF=\frac{Jmax\ x\ \mathrm{Vmax}}{Jsc\ x\ \mathrm{Voc}}$$

Thus maximum power (P_{max}) can be calculated as following formula

$$P_{max}=J_{max}x\ V_{max}=J_{sc}x\ V_{oc}x\ FF$$

Any parameter affecting the FF will directly affect the P_{max}. Any appliance connected to a solar cell can utilize the maximum power only if it's supply voltage (V) is around V_{max} or in other words: The load resistor $R_l = V_{max}/J_{max}$. If V is greater than V_{max} than current is lost through the ideal diode and shunt resistor (R_{sh}).R_{sh} is simply a quantification of recombination of charge carriers near the donor/acceptor interface. R_s stands for series resistor and it also take account in recombination near electrodes but it is at least one order magnitude lower than the first one. Thus, when voltage is very small R_{sh} is the main resistor which resists the flow of current under external potential. On the other hand $R_s$is mainly stands for the mobility of the charge carriers, electrons through n-type materials, holes through p-type materials. R_s increases when there are traps that diminish the number of charge carriers or other barrier in the medium and it also increase with the travelling distance of charge carriers. Ideally R_{sh} should be infinitely high and R_s should be 0. If this is the case FF will take its maximum value 1.If other way around V is smaller than V_{max} than heating the series resistor would be the reason for power reduction.
In order to quantify the power conversion efficiency(η) equation 1.3 is used:

$$\eta=\frac{Jmax\ x\ \mathrm{Vmax}\ x\ \mathrm{FF}}{Pinc} \qquad \text{Equation 1.3}$$

where P_{inc} stands for the power of incident light. Indeed η is depended on the wavenumber and intensity of incident light, in order to compare a result globally, some standards are taken into account. First incident light should be well defined. Widely used AM 1.5G (Air Mass 1.5 Global) is a standard source which simulates the solar light at

sea level with an oblique angle 48.2deg from the zenith with 1000W/m^2 illumination [31].

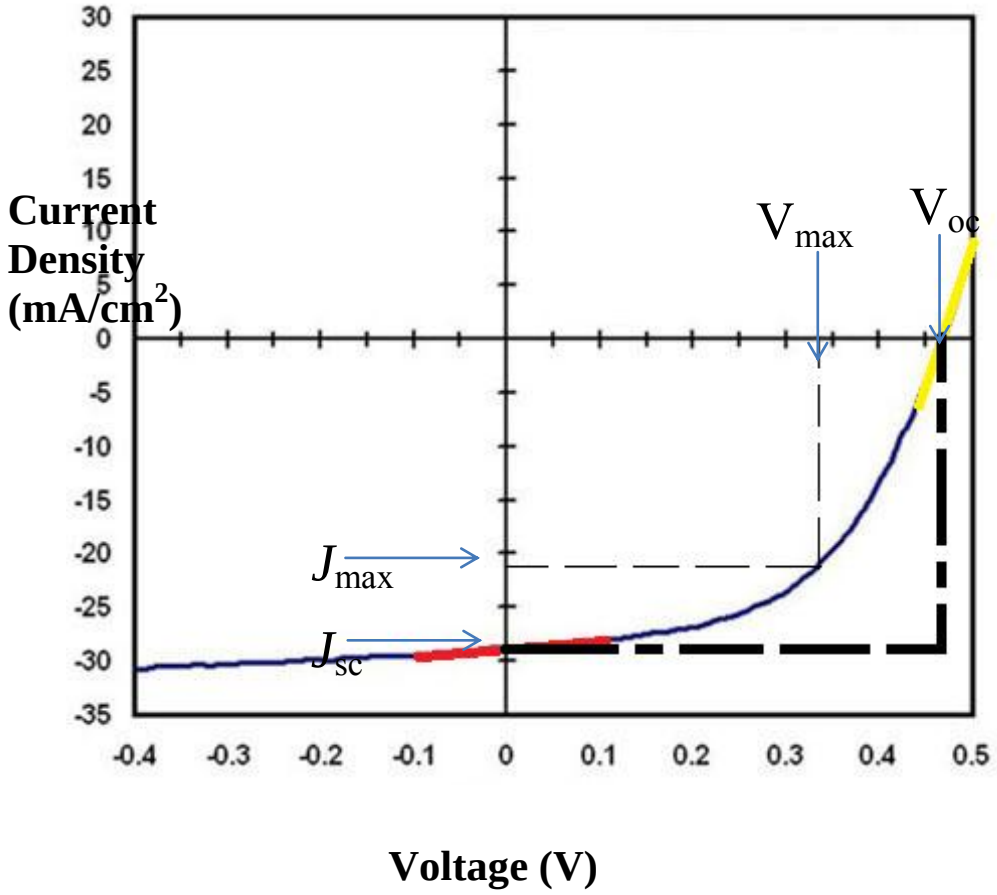

Figure 1.6 Schematic diagram of *J*V curve where slope of red line represents R_{sh} and slope of yellow line represents R_s

1.5 Electrochromism

Chromism is a striking property of a material to sustain different colors under different external effects such as pH, pressure, solvent, potential, temperature and so on. Electrochromism means reversible color change upon external potential. In 1961 theoretical explanation has given by Platt, and the first examples of materials and devices were introduced to literature by Deb [32,33]. Studies among amorphous and crystalline inorganic metal oxides particularly WO_3 as a wide-band-gap material took enormous attention. Metal intercalation to WO_3 leads to formation of strong absorption band in the visible region. Initially transparent WO_3 in the visible region, become a cathodically coloring material M_xWO_3 (where M can be alkali metal or Hydrogen) after reduction. Metal oxides were studied for their electrochromic properties and oxides of V,Mo,Nb , and Ti were found to be as cathodically coloring materials and oxides of Ni, Co, and Ir were found to be as anodically coloring materials. Afterwards organic small molecule

known as viologens, took stages. Bipyridiliums (viologens) are transparent instable dicationic state and highly colored stable radical cation can be formed upon one electron reduction. Then composites of small molecules absorbed on mesoporous nanoparticles made by doped metal oxides were studied and show improved results. After the discovery of electrically conductive organic polymer by three legendary scientists who were awarded with Nobel Prize in 2000, polymers were considered to be a shining star of the future [34]. Their flexibility of being solution processable enabling use in bulk heterojunction cell [35] via structural modification and also ease of modification of HOMO, LUMO and most importantly for the chromism and E_g are just few examples of interesting properties. Just after investigation high optical contrast, rapid switching time and multichromic properties were found to be most striking ones.

1.5.1 Doping Process

In the report of Shirakawa, it was stated that electrical conductivity of polyacetylene can be increased several magnitude orders as it is reacted with reducing agent (n-doping) or oxidizing agent (p-doping) [34].

In inorganic materials like silicon, if one silicon atom is replaced with boron which has one less electron in its valence, newly created lattice seek an electron to fill the vacancy, can be considered as a positive hole, (p-type). On the other way around, if phosphorous is replaced, in the lattice there will be an excess of electron (n-type).

In electrochemistry, doping process can established via charge transfer reaction which results in partially oxidized or partially reduced polymer, in contrast to creation of holes or electrons in inorganic one. Doping process can be done chemically with reducing agent (R) or oxidizing agent (O) or electrochemically by applying certain voltage.

In below equations 1.4 and 1.5 chemical and electrochemical p-doping and in equations 1.6 and 1.7 chemical and electrochemical n-doping can clearly be seen respectively.

$$(\pi\text{-polymer}) + O \rightarrow (\pi\text{-polymer})^{+}O^{-} \qquad \text{Equation 1.4}$$

$$(\pi\text{-polymer}) + [Li^{+}(BF_4^{-})]_{solv} \rightarrow [(\pi\text{-polymer})^{x+}(BF_4^{-})_x] + xLi^{+} + xe^{-} \qquad \text{Equation 1.5}$$

$$(\pi\text{-polymer}) + R \rightarrow (\pi\text{-polymer})^{-}R^{+} \qquad \text{Equation 1.6}$$

$$(\pi\text{-polymer}) + xe^{-} + [Li^{+}(BF_4^{-})]_{solv} \rightarrow [(\pi\text{-polymer})_x^{-}(Li^{+})_x] + x(BF_4^{-}) \qquad \text{Equation 1.7}$$

In term of the properties of induced charges, generally chemical and electrochemical doping gives similar results. However, attempts to intermediate level of doping via chemical manner often result in inhomogeneous. For this reason the main advantage of electrochemically doping is the control of doping level, which gives highly reproducible results.

1.5.2 Voltammetry

Voltammetry is one excellent characterization method for conjugated polymers. One can find HOMO and LUMO levels of the polymer and also hysteresis of doping and dedoping processes. Also differences between HOMO and LUMO levels electronic band gap can be calculated. Another special use of voltammetry is the synthesis of polymers via oxidative polymerization or for some kind reductive.

1.5.2.1 Cyclic Voltammetry

In cyclic voltammetry, three-electrode-system is used. Main current flows between working and counter electrodes. Oxidative or reductive reactions take place on working electrode. Reference electrode is just used to define the potential with respect to working electrode. Triangular wave form signal is created by potenstiostat and signal to voltage converter helps us to realize the cyclic voltammogram on the screen. In the cell there are three electrodes and an electrolytic solution that conduct the electricity. Choice of solvent depends on the material that is to be characterized. Since reactions take place on working electrode and polymer is coated on working electrode, solvent should not dissolve polymer. However it should dissolve the salt to be electrolytic. Also solvent should not have chemical or electrochemical activity in the system. In **Figure 1.7** ITO (Indium Tin Oxide) coated glass substrate was used as the working electrode. Therefore substance-polymer- that is to be examined is coated on this electrode. Reference electrode and counter electrode are silver and platinum wires respectively.

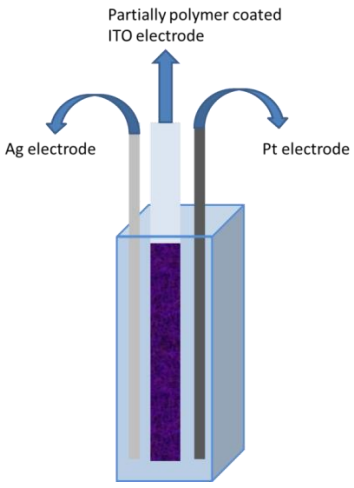

Figure 1.7 Cyclic voltammetry cell

As seen in the **Figure 1.8** oxidation and reduction onset potentials give HOMO and LUMO levels of the species under study, respectively. Zero potential is just a relative number with respect to a reference electrode and exact values should be converted accordingly to a more general reference standard hydrogen electrode to better understand. Electronic band gap (E_g) is just a difference between HOMO and LUMO energy levels.

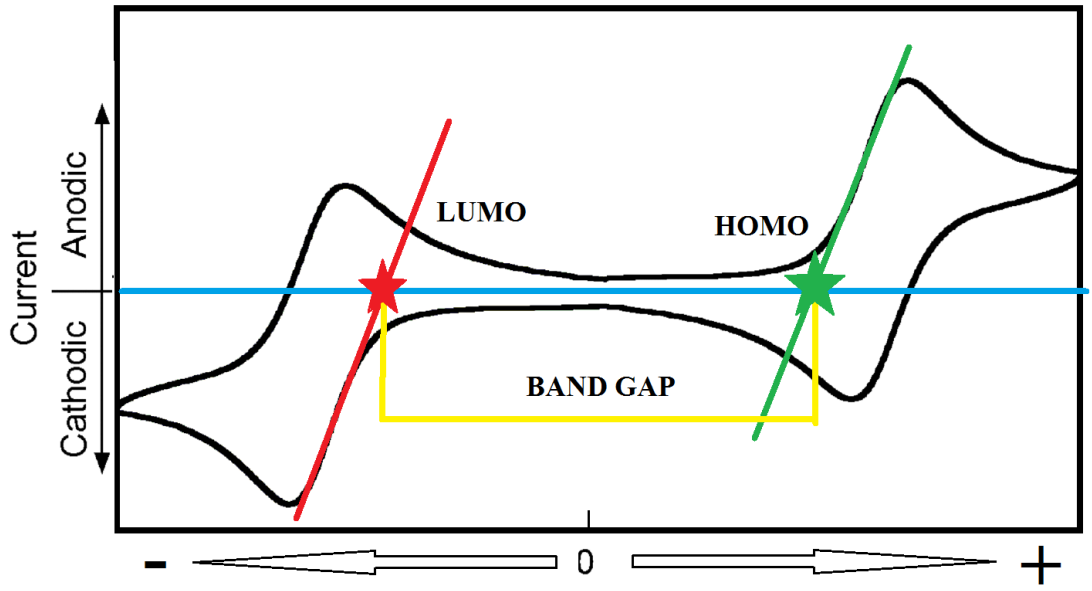

Figure 1.8 Cyclic voltammogram

Moreover, information that can be learned from cyclic voltammetry is not limited to these. The area under the curve is responsible to how much charge a polymer can carry. It is very important for capacitors. One can deduct stability of the polymer. Highlying LUMO level is a sign of oxygen sensitive. As scan rate changes, if current increases according to the Randles-Sevcik equation 1.8 then the reaction takes place -doping/dedoping- is considered as reversible [36]. This reversibility is important for long life time of electrochromic devices.

$$i_p = (2.69 \times 10^5)\, n^{3/2} A D^{1/2} C_i v^{1/2} \qquad \text{Equation 1.8}$$

One other method to see the stability of the electrochromic device is just applying a square wave form as it is in chronoamperometry one can see quantitatively the stability of the material. This is shown in the below **Figure 1.9**.

On the other hand, as it is named electrochromic material should change its color upon applied potential. This change of color can be monitored if electronic absorption spectra is taken out. That can be seen in **Figure 1.10**.

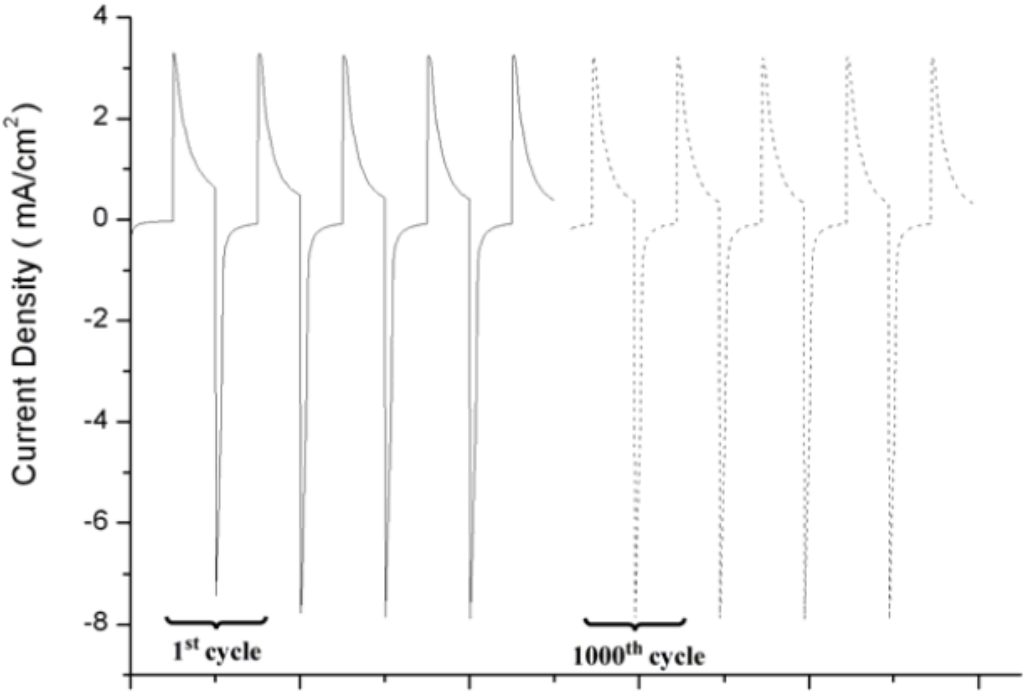

Figure 1.9 Chronoamperometry study to visualize the stability

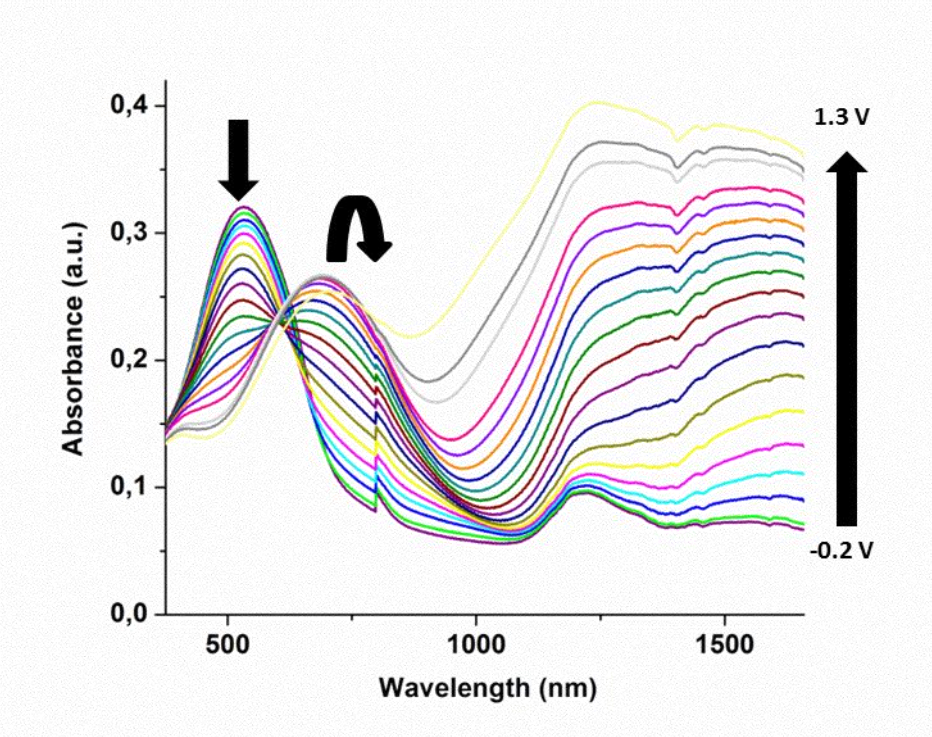

Figure 1.10 Kinetic study to visualize the color change

Aim of ThisWork

The synthesis of novel low bandgap conjugated polymers by tailoring electrochemical andoptical properties is important since application area of the polymers is dependent on these properties. Several strategies were developed for this purpose. The donor–acceptor(DA) theory is simply explained as a combination of donor(electron-rich) and acceptor (electron-deficient) moieties to form a repeating unit in the polymer chain. Recent studies showed that the performance of the solar cells can be improved by developing DA type semiconductors. The organic solar cell (OSC) based on bulk heterojunction with a proper DA approach has made significant progress and power conversion efficiency (PCE) of 8–9% was reported [37].

Among the acceptor units, benzotriazole (BTz) is one of the analog of benzazoles and recently used in electrochromic and photovoltaic applications [38].BTz-based conjugated polymers showed superior properties in electrochromic application. Most of the BTz derivatives switch between multicolored and highly transmissive states that are very important parameters for single component electrochromic devices. Therefore, different donor moieties were selected to couple with BTz to improve the properties of the conjugated polymers and the properties of the polymers were developed in terms of processability, optical contrast, and switching times [38].

Although BTz-based polymers commonly used in electrochromic applications, OSC applications are limited due to low electron accepting property when compared with benzothiadiazole, it leads to high lowest unoccupied molecular orbital (LUMO) energy level and high band gap. However, recent studies in literature proved that OSC having high PCE can be achieved by clever structural modifications [39]. In addition to these properties, BTz-based conjugated polymers are solution processable and suitable material to couple with fused structures. Fused structures are commonly used for OSC and organic field effect transistors (OFET)applications not only to enhance the effective conjugation of the polymer backbone but also to facilitate the delocalization of p-electrons and charge mobility by decreasing rotational disorder [40].Different fused structures were investigated for different applications and the most commonly used fused structures are bithiophene derivatives having different heteroatoms in its structure (nitrogen, carbon, silicon, germanium, and sulfur).Dithienothiophene (DTT) is one of the bithiophene derivative that is preferred in OSCs and OFET applications [41].

The reason why this structure is used in these applications is its attractive properties like higher electron delocalization than thiophene and great aromatic resonance energy disruption due to the higher energy quinoidal states. However, incorporating DTT leads to dramatic decrease in the solubility, and so different synthetic methodologies were developed to handle this problem. Incorporating alkyl chains into the DTT moiety or coupling with structures having alkyl chain can be the solutions for this problem. In this study, due to the aforementioned properties and lack of inventory of BTz- and DTT-containing conjugated polymers, we synthesized low band gap polymers; poly(4-

(dithieno[3,2-b:20,30-d]thiophen-2-yl)-2-(2-octyldodecyl)-2H-benzo[d][1,2,3]-triazole) **P1** and poly(4-(5-(dithieno[3,2-b: 20,30-d]thiophen-2-yl)thiophen-2-yl)-2-(2-octyldodecyl)-7- (thiophen-2-yl)-2H-benzo[d][1,2,3]triazole) **P2** via Stille coupling. Solubility problems of polymers were meliorated by substituting 2-octyl dodecyl unit on the 2-position of the BTz. Optical and electrochemical studies were performed by means of ultraviolet(UV)–visible (Vis) spectrometer and cyclic voltammetry(CV).

CHAPTER 2

EXPERIMENTAL

2.1 General

All chemicals and solvents to synthesize copolymers **P1** and **P2** are shown in **Scheme 2.1** and were purchased from Aldrich and used without any further purification. Tributyl(thiophen-2-yl)stannane (**2**) [42] and 2,6-bis(tributylstannyl)dithieno[3,2-b:20,30-d]thiophene (**3**) [43] and 4,7-dibromo-1H-benzo[d][1,2,3]triazole (**4**) [44] were synthesized with a same methodology described in the literature. Tetrahydrofuran (THF) was freshly dried over sodium and benzophenone just before the reactions and others were used as received. Reactions were performed under nitrogen atmosphere unless otherwise mentioned. Structures of monomers and polymers were proven by NMR recorded on a Bruker Spectrospin Avance DPX-400 Spectrometer with TMS as the internal reference. Molecular weights of the polymers were measured by Gel Permeation chromatography (GPC) on Polymer Laboratories GPC 220 with polystyrene as the standard and THF as the solvent. Thermal properties of the polymer were analyzed by Thermal Gravimetric Analysis (TGA) (Perkin Elmer Pyris 1 TGA) under nitrogen atmosphere at a heating rate of 10 ^{o}C/min. Electrochemical studies were performed using a Voltalab 50 potentiostat in a three electrode cell consisting of an Indium Tin Oxide coated glass slide (ITO) as the working electrode, platinum wire as the counter electrode, and Ag wire as the pseudo reference electrode calibrated against Fc/Fc^{+} (0.3 V). The electrolytes used were 0.1 M of $TBAPF_6$ in acetonitrile (ACN). Highest occupied molecular orbital (HOMO) and lowest lying molecular orbital (LUMO) energy levels were calculated by taking Normal Hydrogen Electrode (NHE) value as -4.75 eV with the formula of HOMO= $-(4.75+0.3+E_{ox}^{onset})$ and LUMO= $-(4.75+0.3+E_{red}^{onset})$. Spectroelectrochemical studies of polymers were carried out by Varian Cary 5000 UV–Vis spectrophotometer and Colorimetry studies were performed via Minolta CS-100 spectrophotometer. The color changes were investigated by colorimetry using the CIE 1931 Yxy color space. Photovoltaic devices were prepared in the following order. ITO(Indium-tin oxide) coated glass substrates were etched partially, in order to take contact. Then substrates were sonicated in three solvents toluene, acetone, isopropyl alcohol. Moreover plasma cleaning was performed. PEDOT:PSS (polyethylenedioxythiophene: polystyrenesulfonate) was coated at 5000 rpm by spin coating onto the clean ITO substrates. Polymer:PCBM mixture were prepared as 2% and 3% in different solvents such as chloroform and chlorobenzene, and coated onto the PEDOT:PSS layer at various rates (750 rpm- 2500 rpm). LiF (0.6 nm) and Al (100 nm) were evaporated onto the polymer at 10^{-7} mbar. Photovoltaic performances of devices were studied in glove-box system (O_2<0.1 ppm, H_2O<0.1ppm) under 1.5G illumination (100 mV/cm^2).

2.2 Synthesis

The synthetic route of **P1** and **P2** is depicted in **Scheme 2.1**. Branched alkyl chain was substituted to the 2- position of the benzotriazole to overcome the solubility problems that is the result of the incorporating fused structures into the polymer chain. 2-octyldodecanol was brominated with PPh_3 and Br_2. Indirect method for the synthesis of **5** was preferred due to the high yield and easy purification of the compound. As outlined in **Scheme 2.1**, synthesis was started with the bromination of benzothiodiazole and was followed by the reduction with $NaBH_4$ in ethanol. Cyclization 3, 6-dibromobenzene-1, 2-diamine to the **4** was performed in the presence of $NaNO_2$ under acidic condition. Desired product **5** was afforded with the yield of 40 %. **5** was reacted with tributyl(thiophen-2-yl)stannane via Stille coupling to synthesize compound **6**. Bromination of compound **6** with N-bromosuccinimide yielded compound **7**. Polymerization of **5** and **7** was performed by Stille coupling with **3**.

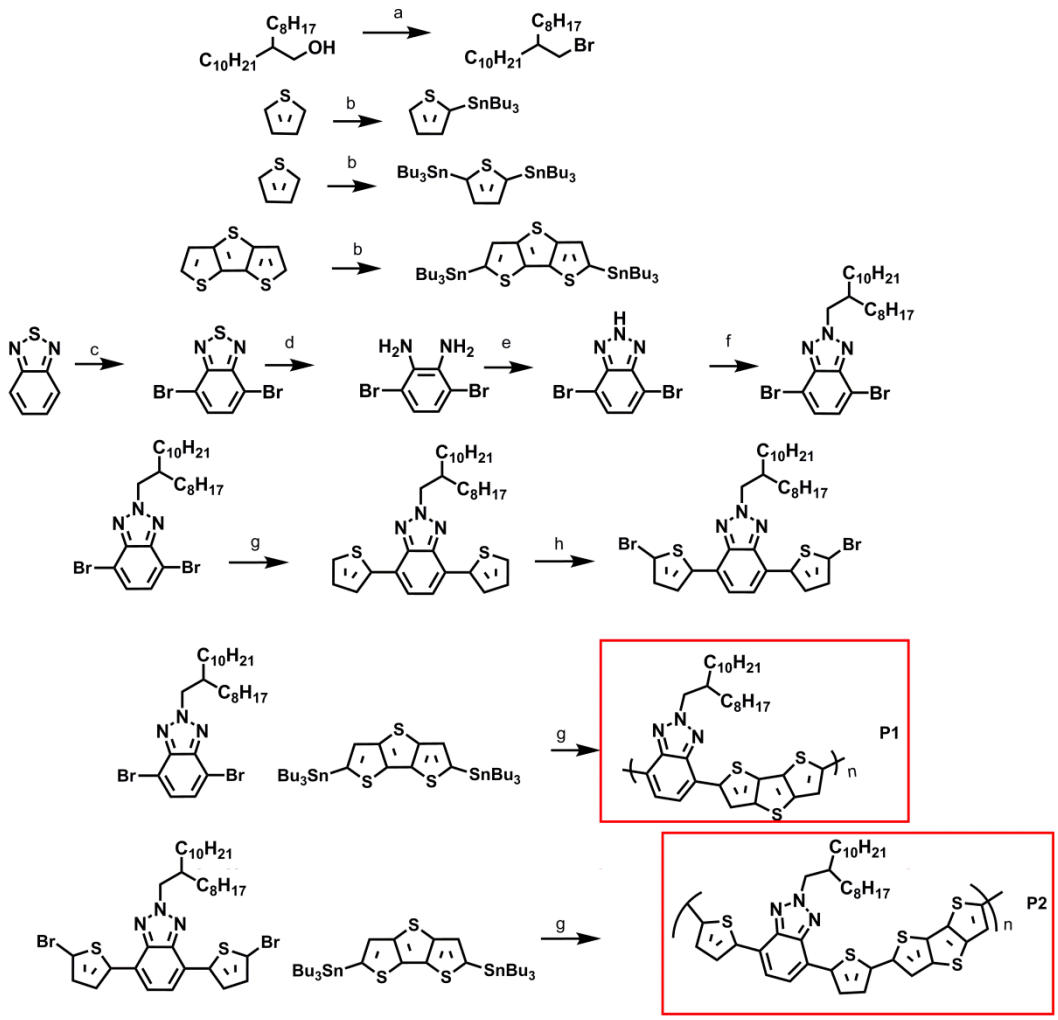

Scheme2.1. Synthetic route of **P1** and **P2** (a- PPh_3, Br_2,CH_2Cl_2 b- Bu_3SnCl, n-BuLi, THF, c- Br_2, C_2H_5OH, d- C_2H_5OH, $NaBH_4$, e- $NaNO_2$, H_2O, AcOH, f- NaH, DMF, g- $Pd(PPh_3)_2Cl_2$, THF h- NBS, DMF)

2.2.1 9-(Bromomethyl)nonadecane (1)

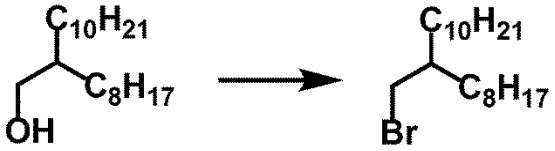

Scheme 2.2 Synthesis of 9-(bromomethyl)nonadecane (**1**)

9-(Bromomethyl)nonadecane was synthesized from its alcohol derivative. 1.94 g (6.5 mmol) 2-octyldodecanol was dissolved in 50 ml CH_2Cl_2. 1.79 g (6.825 mmol) PPh_3 was added to the solution at 0 ^oC. 348 µl (15.4mmol) Br_2 was added and stirred for half an hour at that temperature. Then the reaction was stirred for another half an hour at room temperature. After reaction was completed (TLC) mixture was poured into separatory funnel with 50 ml saturated $NaHSO_3$ then organic part was washed with distilled water and brine and then dried over $MgSO_4$. Organic part was filtered and solvent was evaporated under reduced pressure. White solids are obtained and product was chromatographed on silica gel with hexane as the eluent to yield 2,23 g (95% yield) **1** as colorless oil. ^1H NMR (400 MHz, $CDCl_3$), δ (ppm): 3.37(d, *J*=4.7 Hz, 2H), 1.52 (m,1.46-1.57, 1H), 1.20 (m,1.15-1.32, 32 H), 0.81(t, *J*=6.58 Hz , 6H).^{13}C NMR (100 MHz, $CDCl_3$), δ (ppm): 39.6, 39.5, 32.59, 31.9, 29.8, 29.7, 29.6, 29.5, 29.4, 29.3, 26.6, 22.7, 14.1.

In **Figure2.1** the doublet at 3.37 pm waskept track of for a remark of -CH_2 bonded to Br.

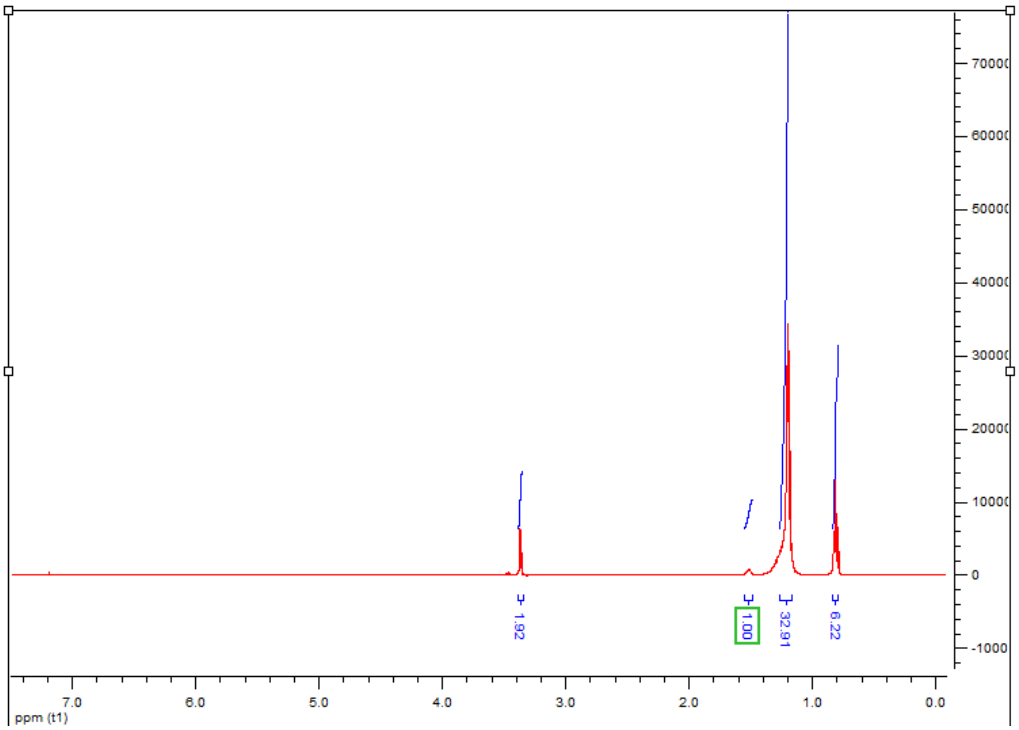

Figure 2.1 ^{1}H NMR spectrum of 9-(bromomethyl)nonadecane **(**1**).**

In **Figure 2.2**, number of carbon atoms was investigated but of course the overlapped peaks are observed.

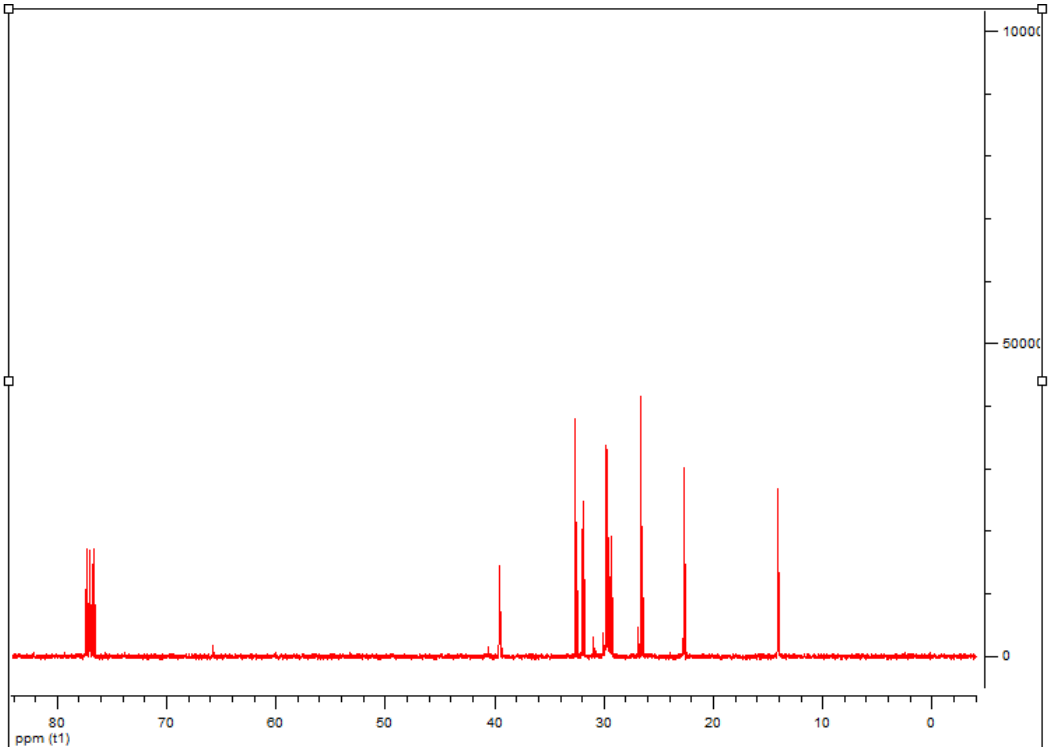

Figure 2.2 ^{13}C NMR spectrum of 9-(bromomethyl)nonadecane (**1**).

2.2.2 4,7-Dibromo-2-(2-octyldodecyl)-2H-benzo[d][1,2,3]triazole (5)

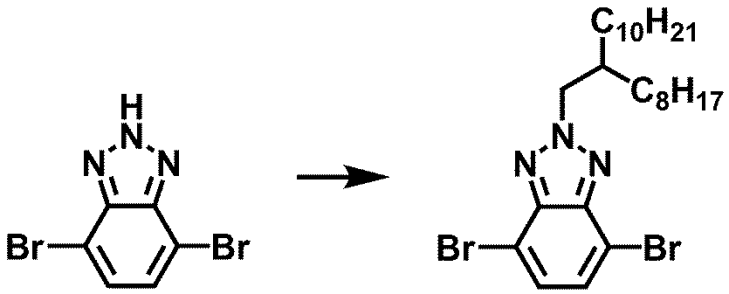

Scheme 2.3 Synthesis of 4,7-dibromo-2-(2-octyldodecyl)-2H-benzo[d][1,2,3]triazole **(5).**

4,7-Dibromo-1H-benzo[d][1,2,3]triazole (**4**) (2 g ,7.22 mmol) was added into 10 ml of DMF and NaH (0.21 g, 8.75 mmol) was added at 0 ^{o}C. Then reaction was completed by adding **1** into the reaction medium. Then reaction was stirred room temperature overnight. After removal of the solvent by evaporation, the residue was dissolved in ethyl acetate and extracted with water. The organic extract was dried over $MgSO_4$ and the solvent was evaporated under reduced pressure. Column chromatography was performed by silica gel with dichloromethane: Hexane (1:2, V: V). 1.4 g (34%) product

was obtained as pale yellow oil. ^{1}H NMR (400 MHz, $CDCl_3$), δ (ppm): 7.32 (s,2H), 4.59 (d, *J*=7.3 Hz, 2H), 2.25 (m,2.19-2.30, 1H), 1.13(m, 1.08-1.30, 32H), 0.78 (m, 0.75-0.80,6H). ^{13}C NMR (100 MHz, $CDCl_3$), δ (ppm):141.4, 127.2, 107.8, 58.9, 36.8, 29.7, 29.6, 29.4, 29.0, 27.6, 27.4, 27.3, 27.2, 27.1, 27.0, 23.8, 20.5, 20.4, 11.9.

In **Figure 2.3,** low field doublet (4.59 ppm/ -CH_2 bonded to N) and low field multiplet (2.19-2.30 ppm/ -CH bonded to N-CH_2-) were expected to be seen.

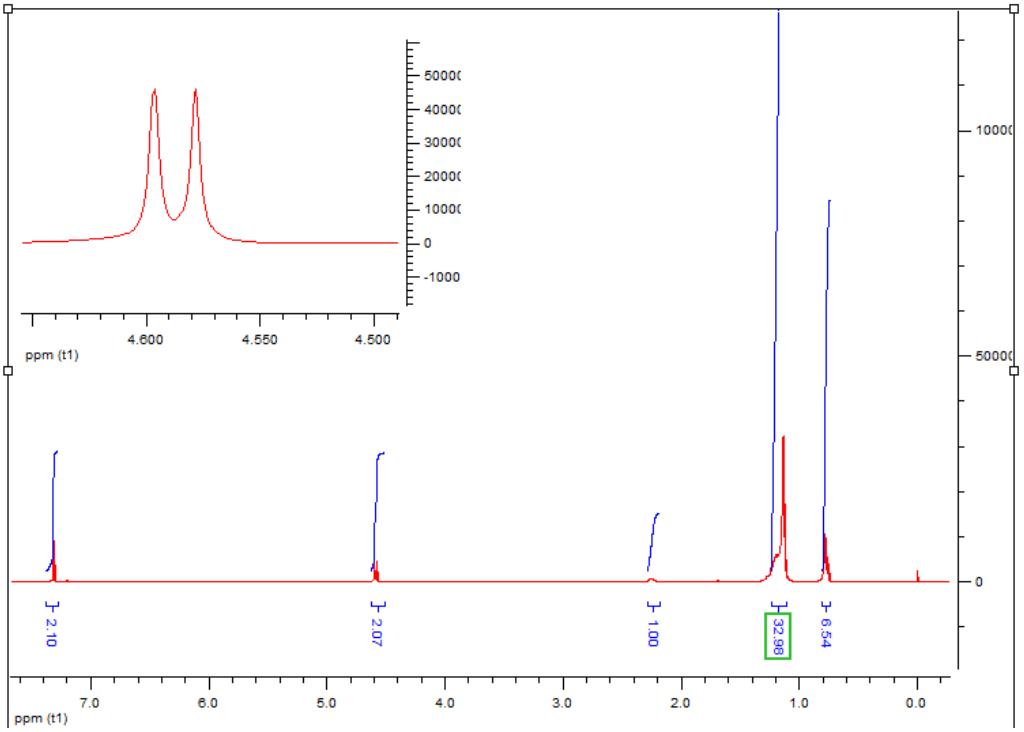

Figure 2.3 ^{1}H NMR spectrum of 4,7-dibromo-2-(2-octyldodecyl)-2H-benzo[d][1,2,3]triazole **(5).**

In **Figure 2.4,** low field aromatic carbon signals belong to benzotriazole, high field carbon signals belong to alkyl chain as expected. Again, overlaps disturbed the calculation of carbon atoms.

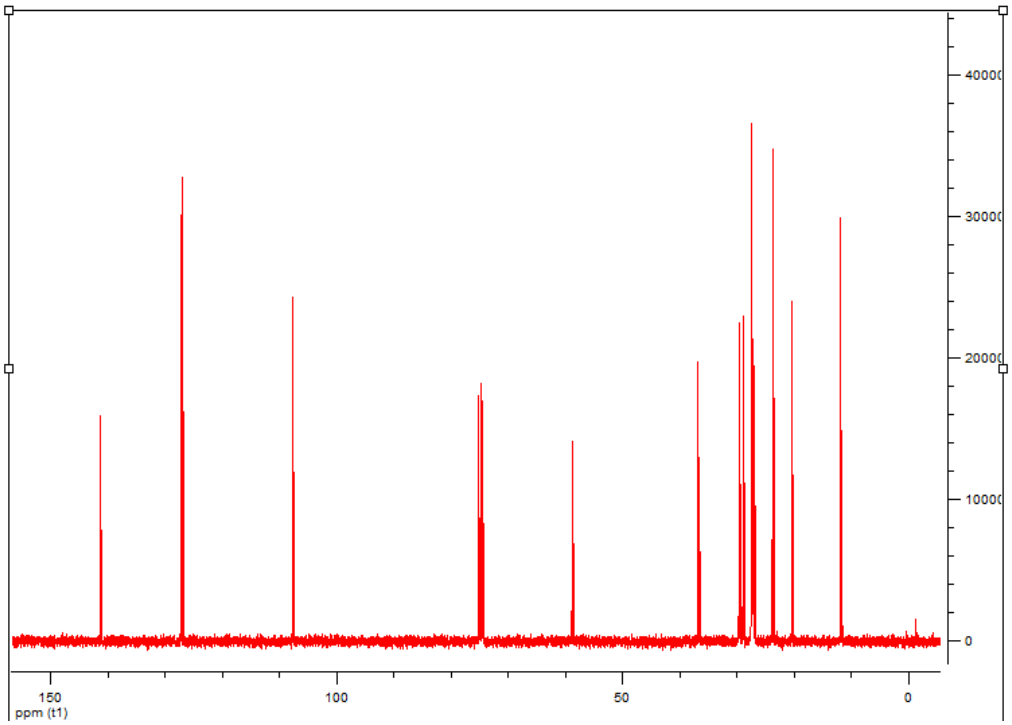

Figure 2.4 ^{13}C NMR spectrum of 4,7-dibromo-2-(2-octyldodecyl)-2H-benzo[d][1,2,3]triazole **(5).**

2.2.3 2-(2-Octyldodecyl)-4,7-di(thiophen-2-yl)-2H-benzo[d][1,2,3]triazole (6)

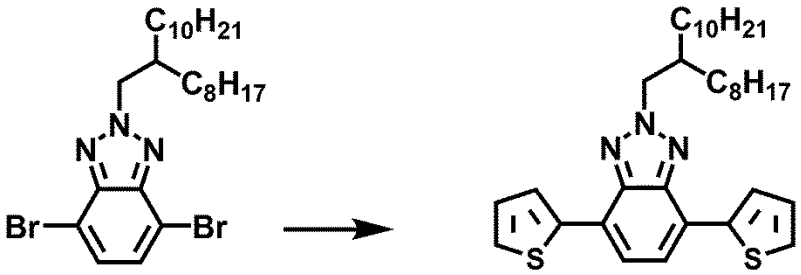

Scheme 2.4 Synthesis of 2-(2-octyldodecyl)-4,7-di(thiophen-2-yl)-2H-benzo[d][1,2,3]triazole**(6).**

5 (1g, 1.8 mmol)and **2** (2.62 g, 3.96 mmol) were dissolved in THF (100 ml) and bis(triphenylphosphine)palladium(II)dichloride (catalytic amount) was added into the solution and reaction was refluxed overnight. After reaction was complete solvent was removed by evaporation. Residue was dissolved in $CHCl_3$ and extracted with water. Organic extract was dried over $MgSO_4$ and solvent was evaporated. Column chromatography was performed by silica gel and product was obtained as green-yellow

solid (70%). ^{1}H NMR (400 MHz, $CDCl_3$), δ (ppm): 8.03 (dd, J_1=1.12 Hz, J_2= 3.67 Hz, 2H), 7.56 (s, 2H), 7.3 (dd, J_1=1.12 Hz, J_2=5.08 Hz, 2H), 7.11 (dd, J_1=5.08 Hz, J_2=3.67 Hz, 2H), 4.67 (d, J=6.63 Hz, 2H), 2.25(m, 2.19-2.30, 1H), 1.25 (m, 1.12-1.38, 32H), 0.8 (m, 0.76-0.83, 6H). ^{13}C NMR (100 MHz, $CDCl_3$), δ (ppm):138.2, 126.2, 125.1, 123.7, 121.8, 120.8, 37.3, 30.1, 30.0, 29.7, 28.1, 27.8, 27.7, 27.5, 27, 27.5, 24.5, 20.8, 12.3.

In**Figure 2.5**, hydrogens on the thiophene rings were expected to be seen in consistent with the number of hydrogen bonded to benzotrizaole and its alkyl chain.

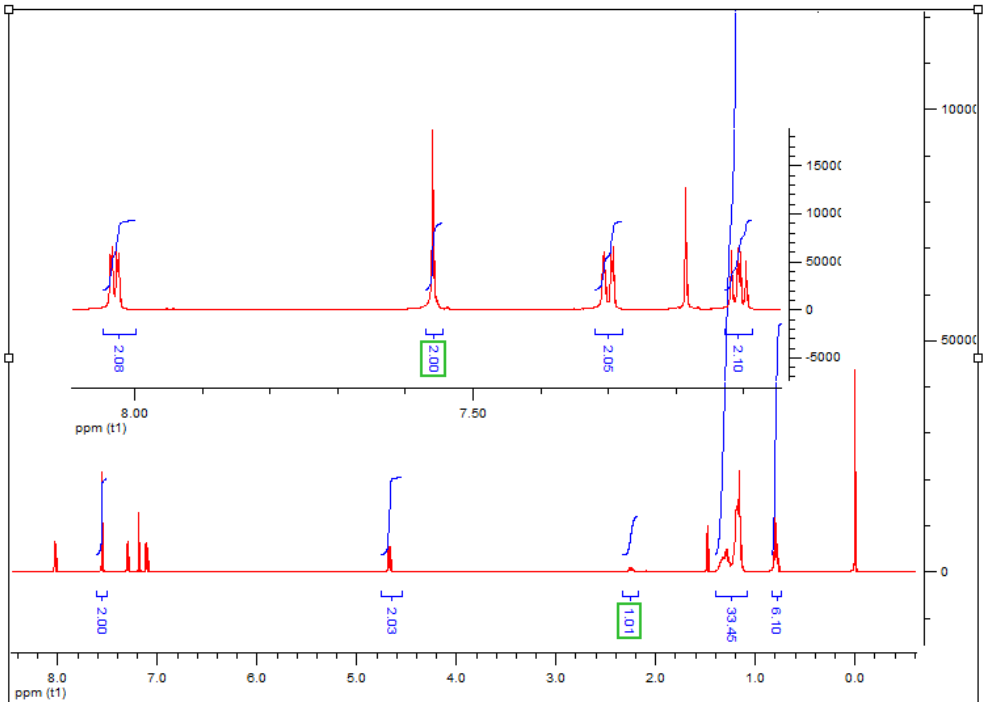

Figure 2.5 ^{1}H NMR spectrum of 2-(2-octyldodecyl)-4,7-di(thiophen-2-yl)-2H-benzo[d][1,2,3]triazole**(6).**

In **Figure 2.6**, due to low signal intensity and overlaps number of carbon atoms could not able tobe quantified but there were aromatic carbons belonging to benzotriazole and thiophenes and aliphatic carbons.

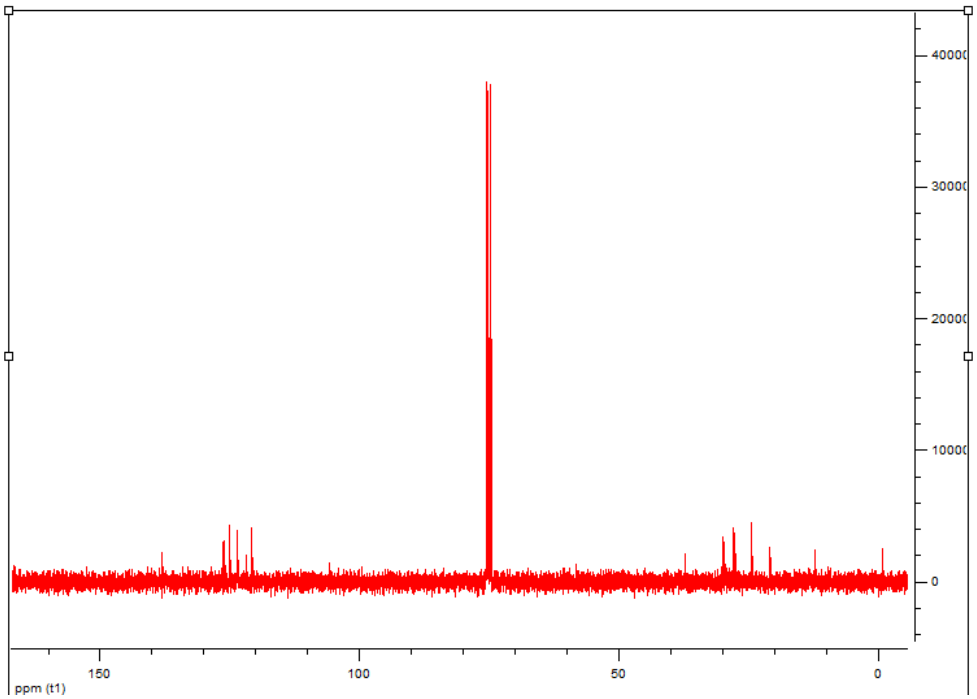

Figure 2.6 ^{13}C NMR spectrum of 2-(2-octyldodecyl)-4,7-di(thiophen-2-yl)-2H-benzo[d][1,2,3]triazole**(6).**

2.2.4 4,7-Bis(5-bromothiophen-2-yl)-2-(2-octyldodecyl)-2H-benzo[d][1,2,3]triazole (7)

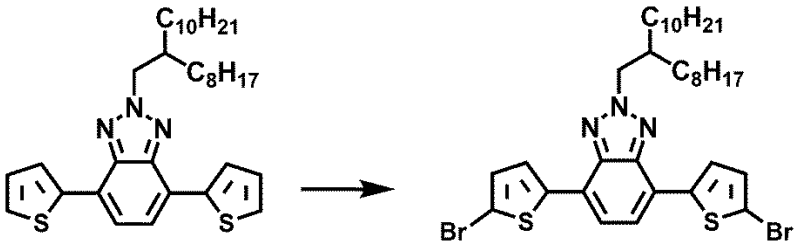

Scheme 2.5 Synthesis of 4,7-bis(5-bromothiophen-2-yl)-2-(2-octyldodecyl)-2H-benzo[d][1,2,3]triazole**(7).**

2-(2-Octyldodecyl)-4,7-di(thiophen-2-yl)-2H-benzo[d][1,2,3]triazole (0.60 g, 1.06 mmol) was dissolved in anhydrous DMF (15 ml), and NBS (456 mg, 2.56 mmol) was added by portion and reaction was protected from sunlight at 80 ^{o}C. Reaction was performed overnight. After reaction was completed extraction with excess water and $CHCl_3$ was done. Organic part was dried over $MgSO_4$ and solvent was removed under reduced pressure. ^{1}H NMR (400 MHz, $CDCl_3$), δ (ppm): 7.70 (d, J=3.96, 2H), 7.42 (s, 2H), 7.04 (d, J=3.96, 2H), 4.64 (d, J=6.54, 2H), 2.20 (m, 2.16-2.27, 1H), 1.2 (m, 1.11-

1.37, 32H), 0.79 (0.76-0.82, 6H). ^{13}C NMR (100 MHz, $CDCl_3$), δ (ppm): 141.6, 141.2, 130.8, 126.8, 122.9, 122.0, 113.1, 59.9, 39.1, 31.9, 31.8, 31.4, 29.9, 29.6, 29.5, 29.3, 29.2, 26.2, 22.3, 14.1.

In **Figure 2.7**, loss of multiplicity of high field hydrogen bonded to thiophene and loss of one hydrogen peak (8.03ppm) were the indicators of the successive bromination.

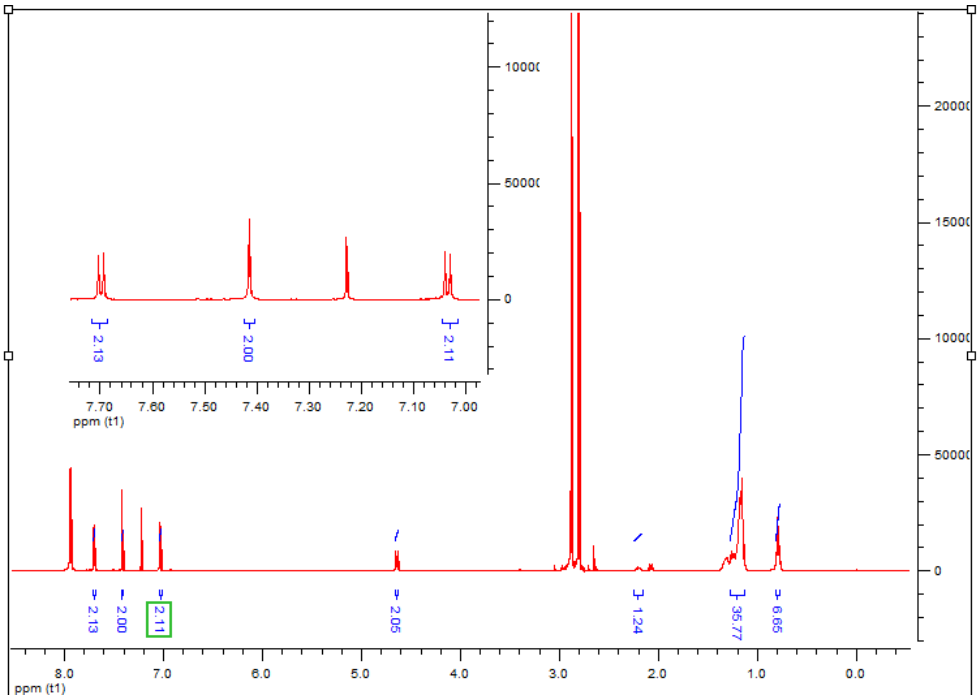

Figure 2.7 ^{1}H NMR spectrum of 4,7-bis(5-bromothiophen-2-yl)-2-(2-octyldodecyl)-2H-benzo[d][1,2,3]triazole **(7).**

In **Figure 2.8**, it was obviously seen that there are seven different aromatic carbon atoms in the molecule and one dominant DMF peak (162.49ppm). Aliphatic carbons were overlapped.

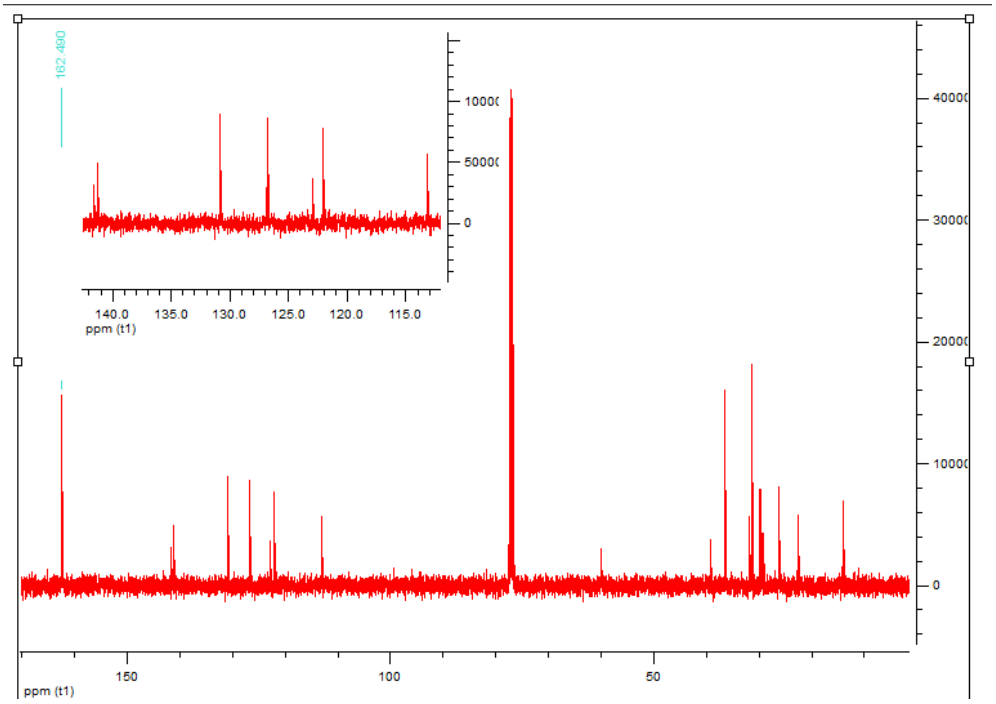

Figure 2.8 ^{13}C NMR spectrum of 4,7-bis(5-bromothiophen-2-yl)-2-(2-octyldodecyl)-2H-benzo[d][1,2,3]triazole **(7).**

2.2.5 Poly(4-(dithieno[3,2-b:2,30-d]thiophen-2-yl)-2-(2-octyldodecyl)-2H-benzo[d][1,2,3]triazole) (P1)

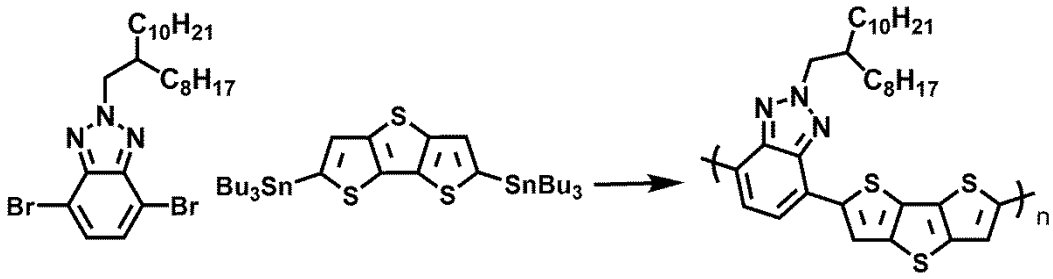

Scheme 2.6 Synthesis of Poly(4-(dithieno[3,2-b:2,30-d]thiophen-2-yl)-2-(2-octyldodecyl)-2H-benzo[d][1,2,3]triazole) **(P1).**

4,7-Dibromo-2-(2-octyldodecyl)-2H-benzo[d][1,2,3]triazole (**5**) (0.318 g, 0.57 mmol) and 2,6-Bis(tributylstannyl)dithieno[3,2-b:20,30-d]thiophene (**3**) (0.443 g, 0.57 mmol) were dissolved in dry THF and bis(triphenylphosphine)palladium(II)dichloride (0.15 g) was added to the reaction mixture and refluxed for 3 days. Bromobenzene and tributyl(thiophen-2-yl)stannane were added into the solution as an end capper. Polymers were precipitated by pouring into methanol and Soxhlett extraction was carried out by methanol, hexane, and acetone, polymer was recovered by chloroform and dried under

vacuum. **P1** was obtained as a purple solid with a yield of 65%. GPC: number average molecular weight (Mn) =38,000, weight average molecular weight (Mw) = 412,000, polydispersity index (PDI) = 11.

^{1}H NMR (400 MHz, $CDCl_3$), d (ppm): 7.37 (BTz), 7.28(BTz), 6.92 (DTT), 6.69 (DTT), 4.59 (N–CH2, BTz), 2.25 (–CH), 1.18(–CH2), 0.78 (CH3).

In **Figure 2.9**, broad peaks were observed as expected.

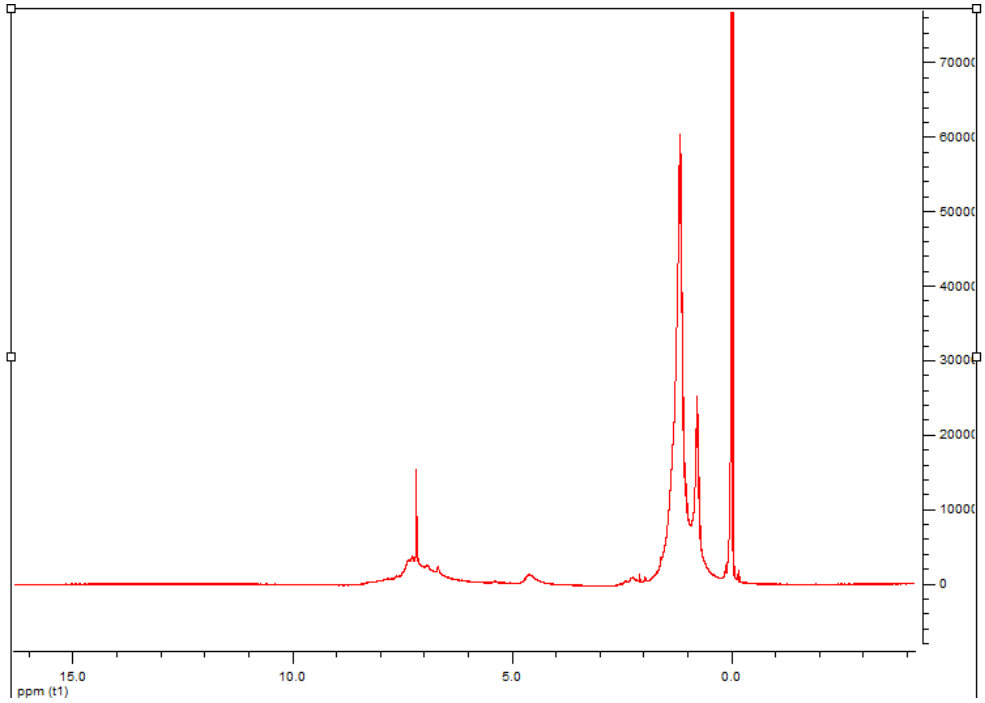

Figure 2.9 ^{1}H NMR spectrum of Poly(4-(dithieno[3,2-b:2,30-d]thiophen-2-yl)-2-(2-octyldodecyl)-2H-benzo[d][1,2,3]triazole) **(P1).**

2.2.6 Poly(4-(5-(dithieno[3,2-b:20,30-d]thiophen-2-yl)thiophen-2-yl)-2-(2-octyldodecyl)-7-(thiophen-2-yl)-2H-benzo[d][1,2,3]triazole) (P2)

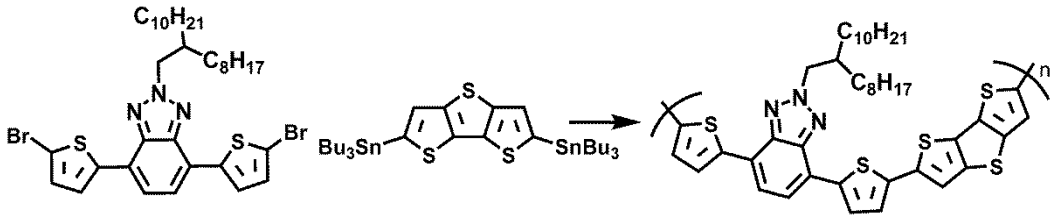

Scheme 2.7 Synthesis of Poly(4-(5-(dithieno[3,2-b:20,30-d]thiophen-2-yl)thiophen-2-yl)-2-(2-octyldodecyl)-7-(thiophen-2-yl)-2H-benzo[d][1,2,3]triazole) **(P2).**

The same procedure was applied using 4,7-bis(5-bromothiophen-2-yl)-2-(2-octyldodecyl)-2H-benzo[d][1,2,3]triazole (**7**) and bis(tributylstannyl)dithieno[3,2-b:20,30-d]thiophene(**3**). **P2** was obtained as red solid with the yield of 48%. GPC: Mn= 4000, Mw = 14,000, PDI = 3.5.

^{1}H NMR (400 MHz, CDCl3), d (ppm): 8.04 (Thiophene), 7.55(BTz), 7.3(DTT), 7.12(DTT), 4.7 (N–CH2, BTz), 2.28 (–CH), 1.20 (–CH2), 0.79 (CH3).

In **Figure 2.10** due to low Mn value **P2** did not give as broad peak as **P1** had.

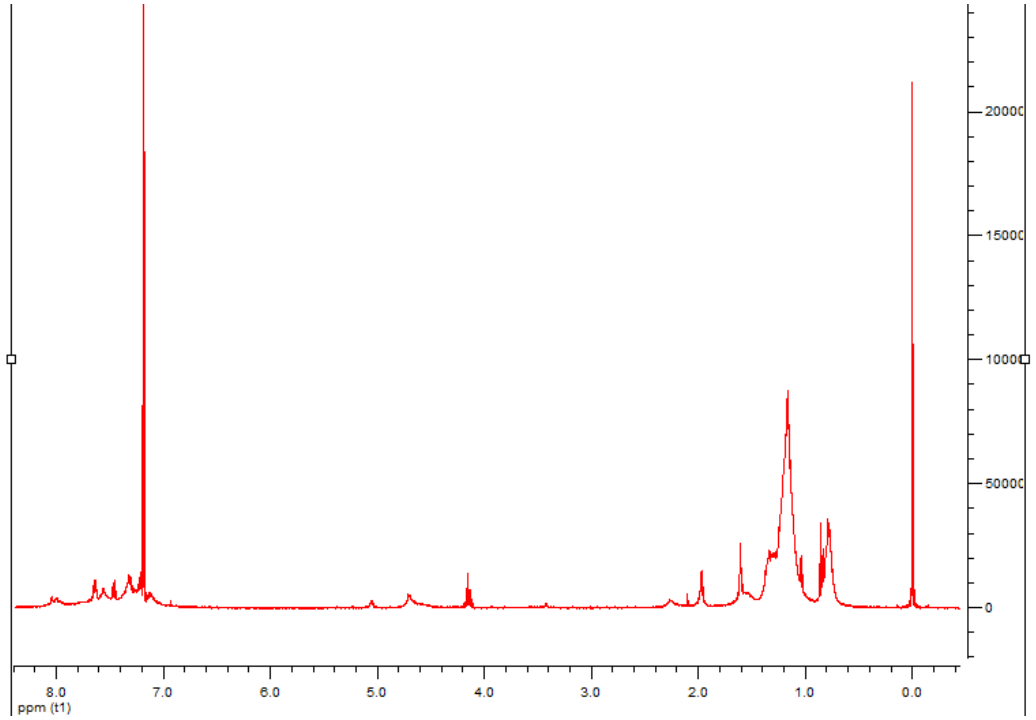

Figure 2.10 ^{1}H NMR spectrum of Poly(4-(5-(dithieno[3,2-b:20,30-d]thiophen-2-yl)thiophen-2-yl)-2-(2-octyldodecyl)-7-(thiophen-2-yl)-2H-benzo[d][1,2,3]triazole) (**P2**).

CHAPTER 3

RESULTS & DISCUSSION

3.1 Optical Studies

The UV–Vis spectra of **P1** and **P2** in chloroform solution and the thin film were shown in **Figure 3.1.** The maxima, onset points, and optical band gaps of polymers were presented in **Table 3.1**. Absorption bands observed in the visible region with maxima of 540 nm and 506 nm were attributed to the π–π* transition of polymers, respectively, **P1** and **P2**. Although **P2** has two more thiophene rings in its structure, an unexpected hyposochromic shift was observed that can be attributed to the repeating units of polymers. Repeating units of the **P2** is low because incorporating of additional two thiophene rings between the BTz and DTT moiety leads to a decrease in solubility thus short conjugation length.

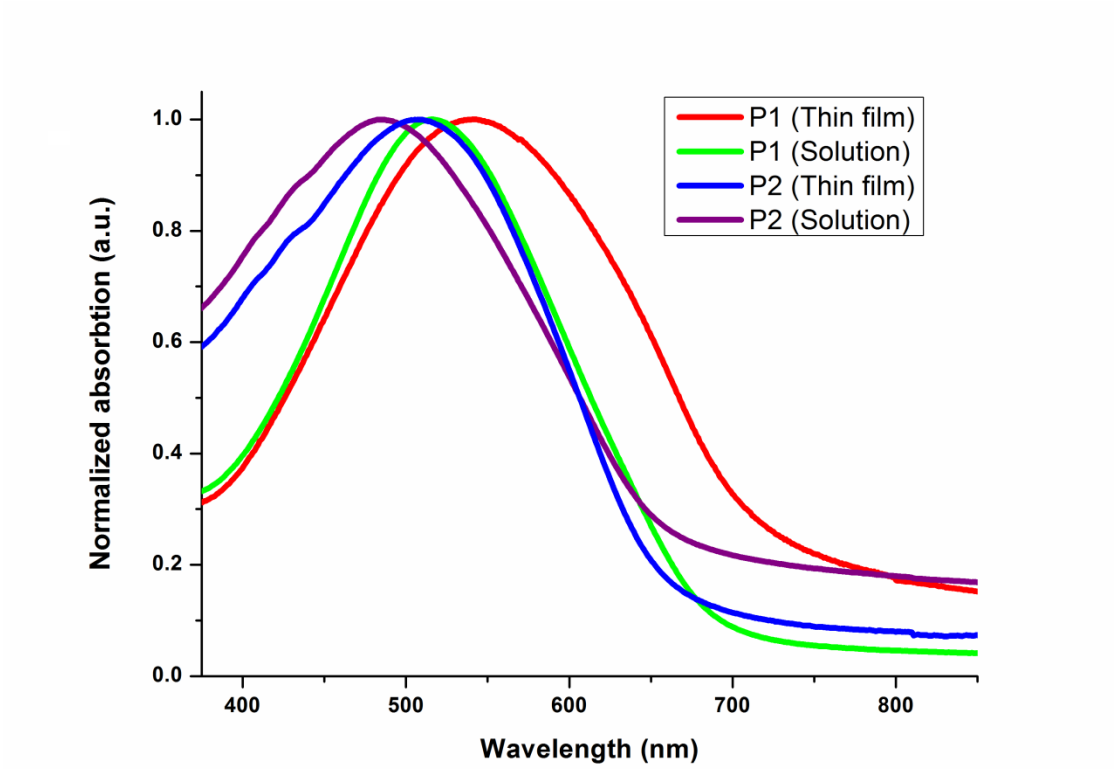

Figure 3.1 Normalized absorption spectra of **P1** and **P2** in thin film and solution**.**

Maxima of **P1** and **P2** in thin film showed a red shift (24 nm and 21 nm red shifted, respectively) in comparison with their solution spectra. These shifts indicate the

aggregation of polymer chains in the solid state due to either a substantial amount of inter chain delocalization or chain planarization in the thin film namely π–π stacking [45].Band gaps of polymers have to be appropriate to harvest solar light effectively. From the onsets of the spectra, the optical band gaps (E_g^{opt}) of polymers **P1** and **P2** were calculated to be 1.78 eV and 1.63 eV, respectively. Band gaps of polymers are suitable for solar cell applications and both polymers had a characteristic band starting from 350 nm with an edge of 700 nm.

TABLE 3.1 Electrochemical and Optical Properties of**P1**and**P2.**

	UV-Vis Absorption Spectra				**Cyclic Voltammetry**				
Polymers	**λ_{max}(nm) Thin film**	**λ_{max}(nm) solution**	**λ_{onset} (nm)**	**E_g^{opt}(e V)**	**E_{ox}/ E_{ox}^{onset} (V)**	**E_{red}/ E_{red}^{onset} (V)**	**HOMO (eV)**	**LUMO (eV)**	**E_g^{ec} (eV)**
P1	540	516	695	1.78	1.03/0. 59	-1.58/ -1.18	-5.64	-3.87	1.77
P2	506	485	760	1.63	1.17/0. 62	-1.68/ -1.23	-5.67	-3.82	1.85

3.2 ElectrochemicalStudies

Convenient band gap of the polymer is not the only crucial parameter for solar cell applications. Proper alignment of the highest occupied molecular orbital (HOMO) and the LUMO energy levels are also critical. Therefore, CV studies were performed to evaluate redox properties and to determine HOMO–LUMO energy levels of polymers. Polymers were dissolved in chloroform (5 mg/mL) and spray coated onto the indium tin oxide (ITO) surface with a thickness of 100 nm for **P1** and 110 nm for **P2**. CV studies were carried out in three-electrode system where an ITO electrode was modified with a polymer film that was used as the working electrode, a platinum (Pt) electrode was served as the counter electrode, and a silver (Ag) wire calibrated against Fc/Fc^+ (0.3 V) was used as the pseudo reference electrode. CV measurements were carried out in 0.1 M $TBAPF_6$ in acetonitrile (ACN) solution at a scan rate of 100 mV/s. Oxidation and reduction voltammograms were depicted in **Figure 3.2**. Both **P1** and **P2** showed p- and n-dopable properties during oxidation and reduction processes. Their corresponding oxidation and reduction couples of **P1** and **P2** were observed at 1.03/0.90 V and 1.17/0.86 V, respectively (**Table 3.1**).

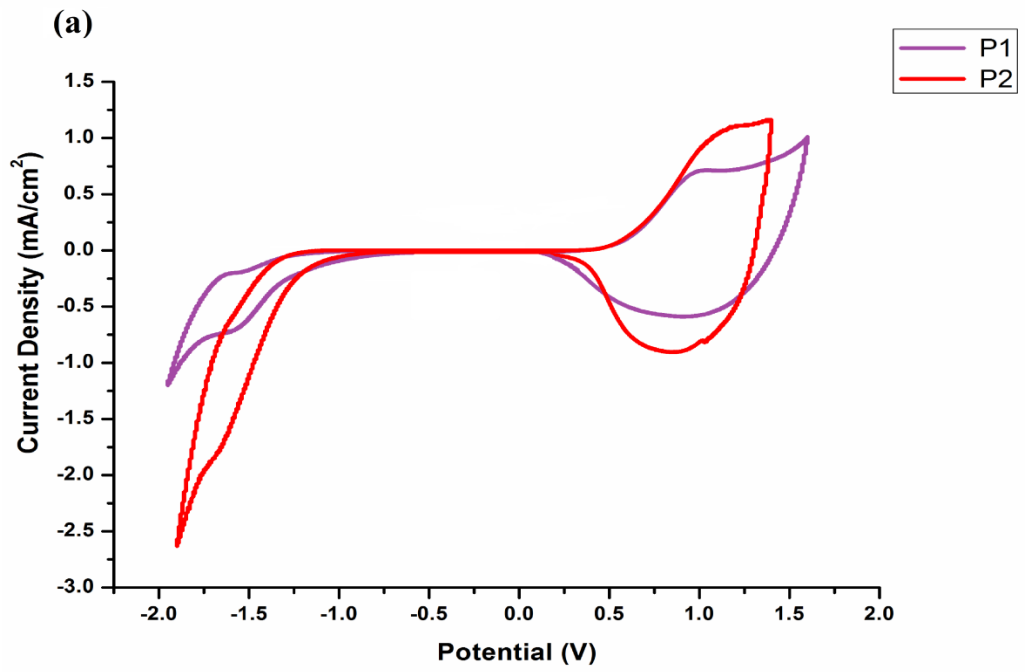

Figure 3.2 Single-scan cyclic voltammograms of **P1** and **P2** on ITO electrode in 0.1 M $TBAPF_6$/ACN

Both HOMO and LUMO energy levels were estimated from the oxidation and reduction onsets. In anodic scan, oxidation onsets of **P1** and **P2** were estimated as 0.54 eV and 0.59 eV. Corresponding HOMO energy levels of **P1** and **P2** were -5.64 and -5.67 eV, respectively. These deep-lying HOMO energy levels ensure the better air stability and high V_{oc} in the device fabrication that is dependent on HOMO energy level of the polymer (donor) and LUMO energy level of the acceptor (PCBM). For the solar cell fabrication, location of the LUMO energy level is crucial to ensure the effective charge separation of the exciton and expected to be 0.3 eV higher than the LUMO energy level of the PCBM. Therefore, reduction onsets of **P1** and **P2** were calculated to be -1.18 and -1.23 eV and LUMO energy levels were determined to be - 3.87 eV for **P1** and - 3.82 eV for **P2** from the cathodic scans. E_g^{ec} (electronic band gap) was higher than the E_g^{opt} (optical band gap) due to the creation of the free charges in CV for **P1**. However, similar trend were not observed for **P2**, energy difference between E_g^{ec} and E_g^{opt} was not seen, this can be attributed to smaller exciton binding energy of the electron [46].It is shown in **Figure 3.3**, The anodic peaks of **P1** and **P2** gradually increase as a linear function of scan rate, which indicates that the electrochemical processes are reversible and non-diffusioncontrolled .

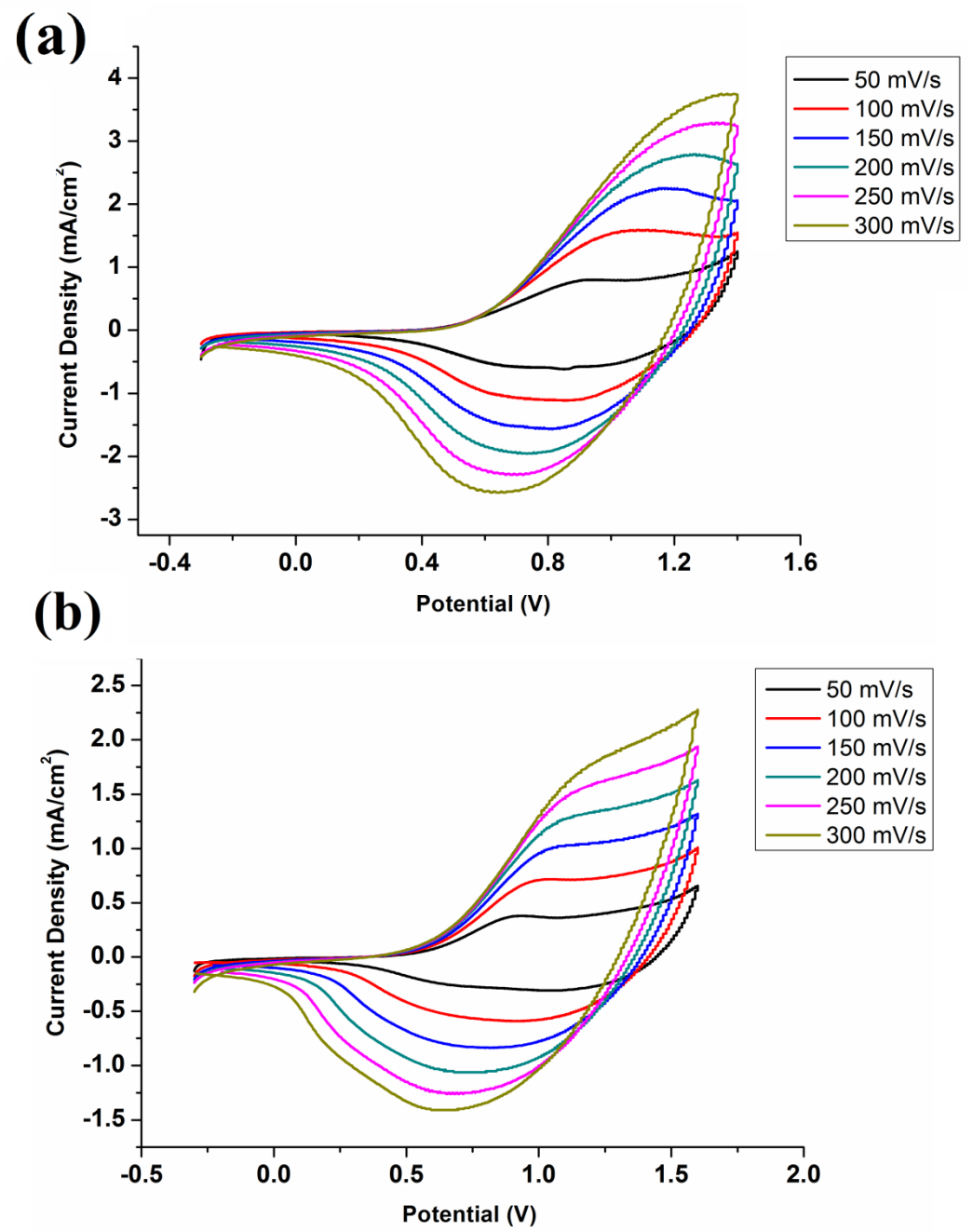

Figure 3.3 Cyclic voltammograms of **P1** (a) and **P2** (b) in 0.1 M $TBAPF_6$/ACN at scan rates of 50, 100, 150, 200, 250, and 300 mV/s.

3.3 Spectroelecrochemistry

Spectroelectrochemistry studies were performed to investigate the change in the optical properties during redox processes. Therefore, spray-coated polymer films were stepwise

oxidized by an external voltage, and spectral responses were recorded using UV–Vis–NIR spectroscopy. Besides, colorimetry measurements were performed to investigate the color change, and International Commission on Illumination (CIE) system having three attributes of color, luminance (L), hue (a), and saturation (b) was used. **P1** revealed a maximum at 530 nm corresponding to the π–π* transition of the polymer. The polymer was purple (L: 51.175, a: 24.082, b: 4.020) in its neutral state. On stepwise oxidation, the absorption at 540 nm diminished and new bands were intensified at around 700 nm (polaron) and 1260 nm (bipolaron). Polaron band was tailed in the Vis region resulted in multichromism and different colors were observed at different potentials. **P1** exhibited black (L: 50.334, a: -5.390, b: 5.346) in its intermediate state and blue (L: 52.286, a: -10.263, b: -23.431) in its oxidized state. Formation of black color is rarely observed for conjugated polymers and significantly important for electrochromic applications, such as smart windows; the breathtaking point was that incremental increases in the potential turn out to be enough to have all seen color in the **Figure 3.4** [47]**P2** showed corresponding maxima due to the π–π* transition at 490 nm. On applied potential intensity of the peak around 490 nm started to decrease and new low-energy bands developed (at 670 and 1350 nm) due to polaronic and bipolaronic charge carriers. Incorporation of the additional electron rich thiophene unit between DTT and BTz affected the doping rate of polymers and more color become detectable for **P2**. **P2** showed red color (L: 52.509, a: 35.270,b: 36.834) in its neutral state and become blue (L: 54.594,a: -6.828, b: -28.278) in its oxidized state. Reduction in neutral polymer films **P1** and **P2** was not resulted in a color changes and **P1** revealed a purple color and **P2** a red color in their reduced states. It is noteworthy to state that both the polymers have the same spectral response on reduction process [48]

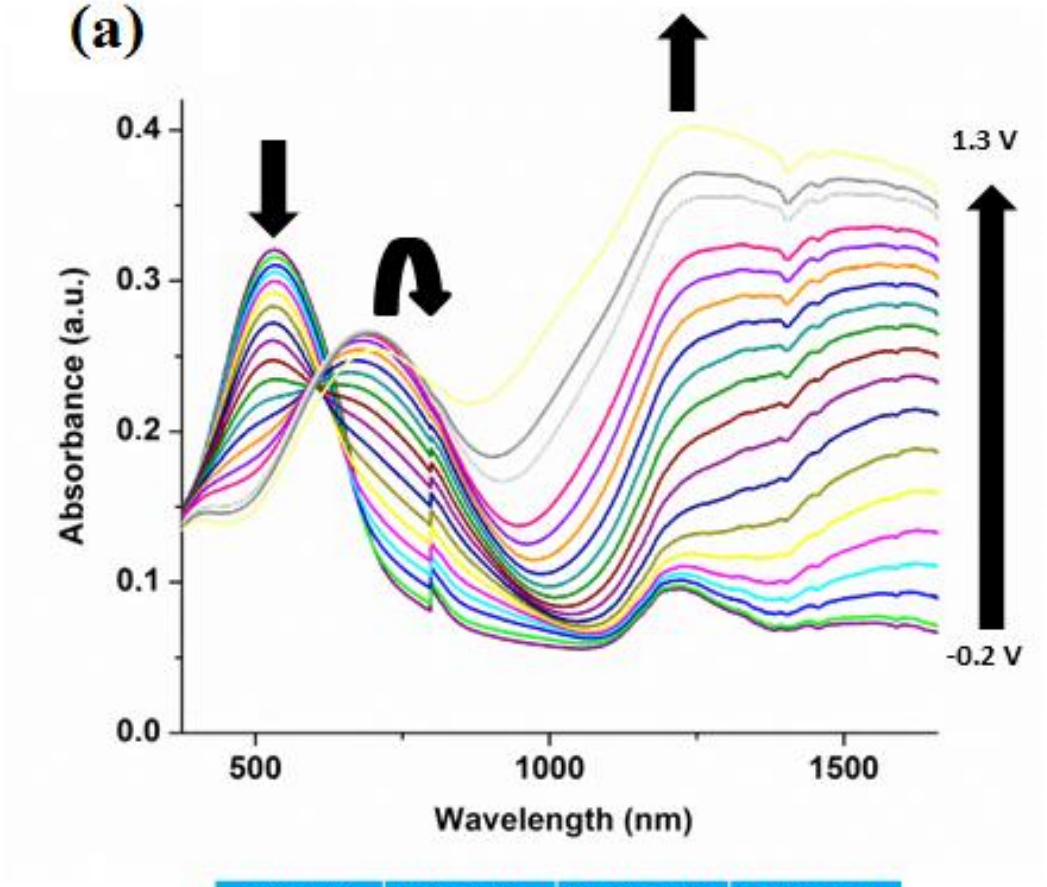

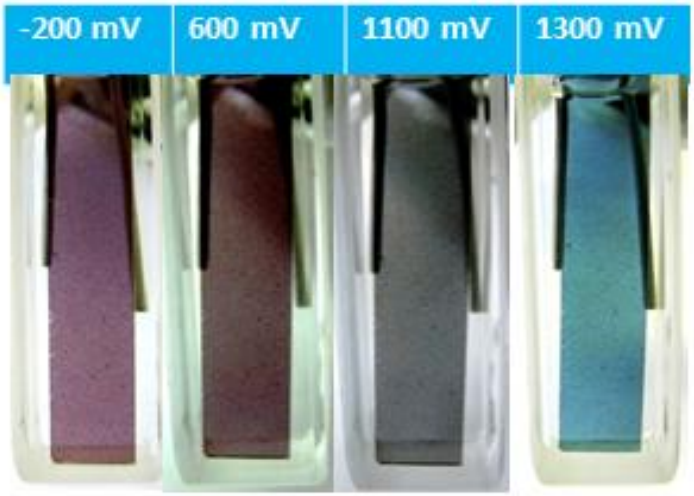

-200 mV	600 mV	1100 mV	1300 mV
L:51.175	L:50.216	L:50.334	L:52.286
a:24.082	a:11.287	a:-5.390	a:-10.263
b:4.020	b:18.419	b:5.346	b:-23.431

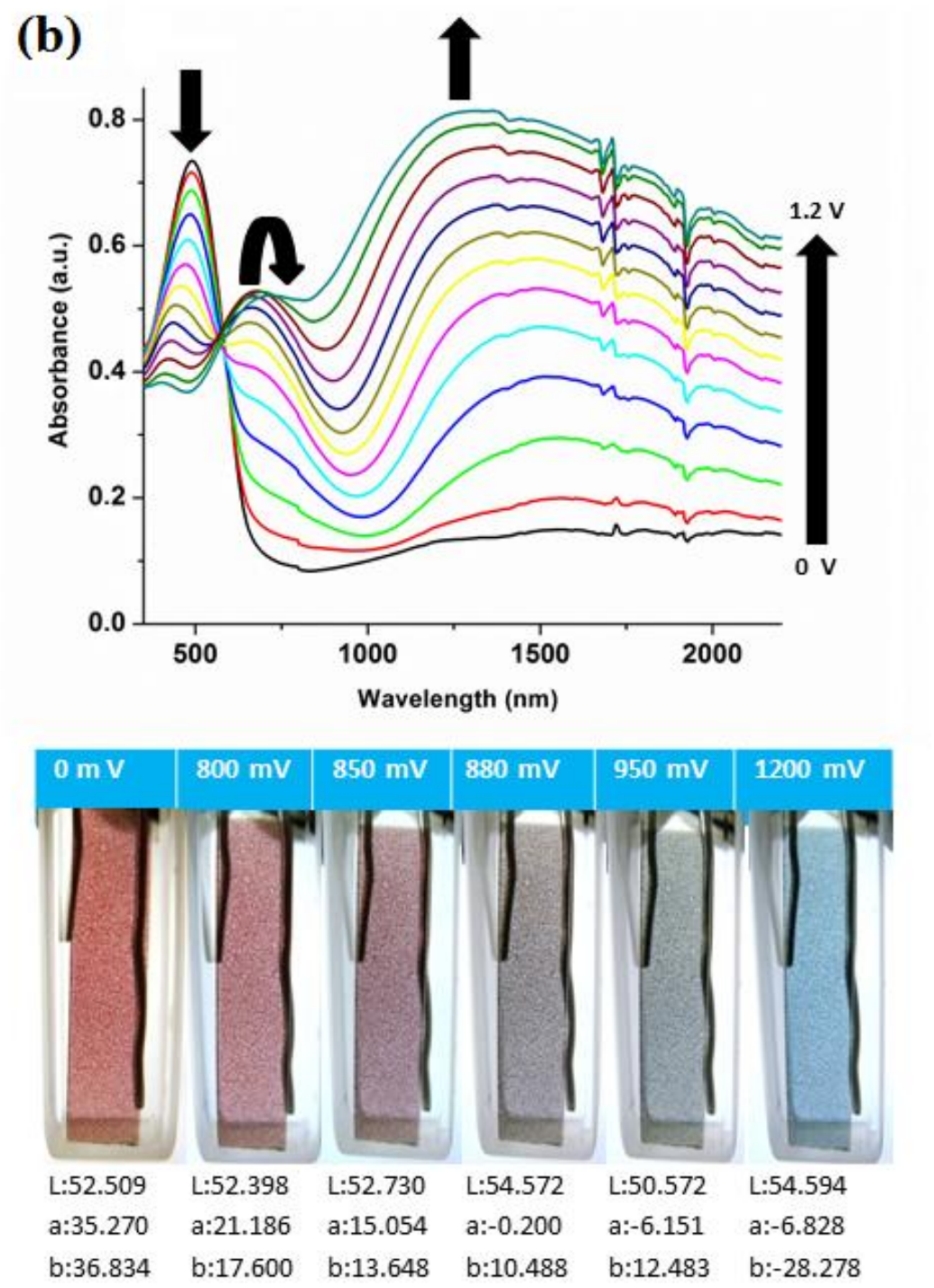

Figure 3.4UV–Vis–NIR absorption spectra of **P1** (a) potential between -0.2 and 1.3 V, **P2** (b) potential between 0 and 1.2 V, and the colors of the respective polymers and their L, a, and b values.

3.4 KineticProperties

Chronoamperometry studies were investigated on an ITO glass slide where the polymers were subjected to potential cycling between their neutral or reduced and oxidized states in0.1 M TBAPF6/ACN solvent/electrolyte couple. Transmittance between two distinct states of polymers has been monitored both in the Vis and NIR region with a time interval of 5 s as shown in the **Figure 3.5**. The optical contrasts and switching times of the polymers are summarized in **Table 3.2**. Optical contrasts of **P1** are 20% at 530 nm, 14% at 700 nm, and 50% at 1260 nm. Optical contrast of the **P2** was higher than **P1**. **P2** revealed satisfactory optical contrasts in the Vis region with 22% at 490 nm, 26% at 670 nm, and in the NIR region with 60% at 1350 nm. Both polymers showed high optical contrast in NIR region, which is a very important parameter for NIR electrochromic device applications such as telecommunication windows, variable optical attenuators, and environmental control (heat gain or loss) system in buildings [49].

TABLE 3.2 Optical Contrast and Switching Times of **P1** and **P2** inVis and NIR Region

Polymers	Optical Contrast (ΔT%)	Switchingtimes (s)
P1	20% (530 nm)	0.9
	14% (700 nm)	0.3
	50% (1260 nm)	0.3
P2	22% (490 nm)	2
	26% (670 nm)	0.6
	60% (1350 nm)	0.9

Switching time is defined as the time required for coloring and the bleaching processes and crucial parameter for dynamic display and switchable mirror applications. **P1** showed fascinating switching times and switched between oxidized and neutral states in 0.9 s (530 nm), 0.3 s (700 nm), and 0.3 s (1260 nm). **P1** showed lower switching timethan **P2**. **P2** is anticipated to have lower switching time than **P1**due to the insertion of additional thiophene units that are expected to improve ion diffusion and dopant insertion. However, the switching time depends on several factors including the ionic conductivity of the electrolyte, magnitude of the applied potential, film thickness, and morphology of the thin film as well as ion diffusion so the observed switching times for **P2** were 2 s (490 nm), 0.6 s (670 nm), and 0.9 s (1350 nm) but its switching times for 670 and 1350 nm were <1 s [50]. Polymers achieved reasonable optical contrast with very fast switching <1 s, although **P2** had one exception 2 s at 490 nm. To the best of our knowledge, rapid switching using reasonable optical contrast made our polymers one of the best candidate for electrochromic devices especially **P1** with 0.3 s at 1260 nm for NIR devices.

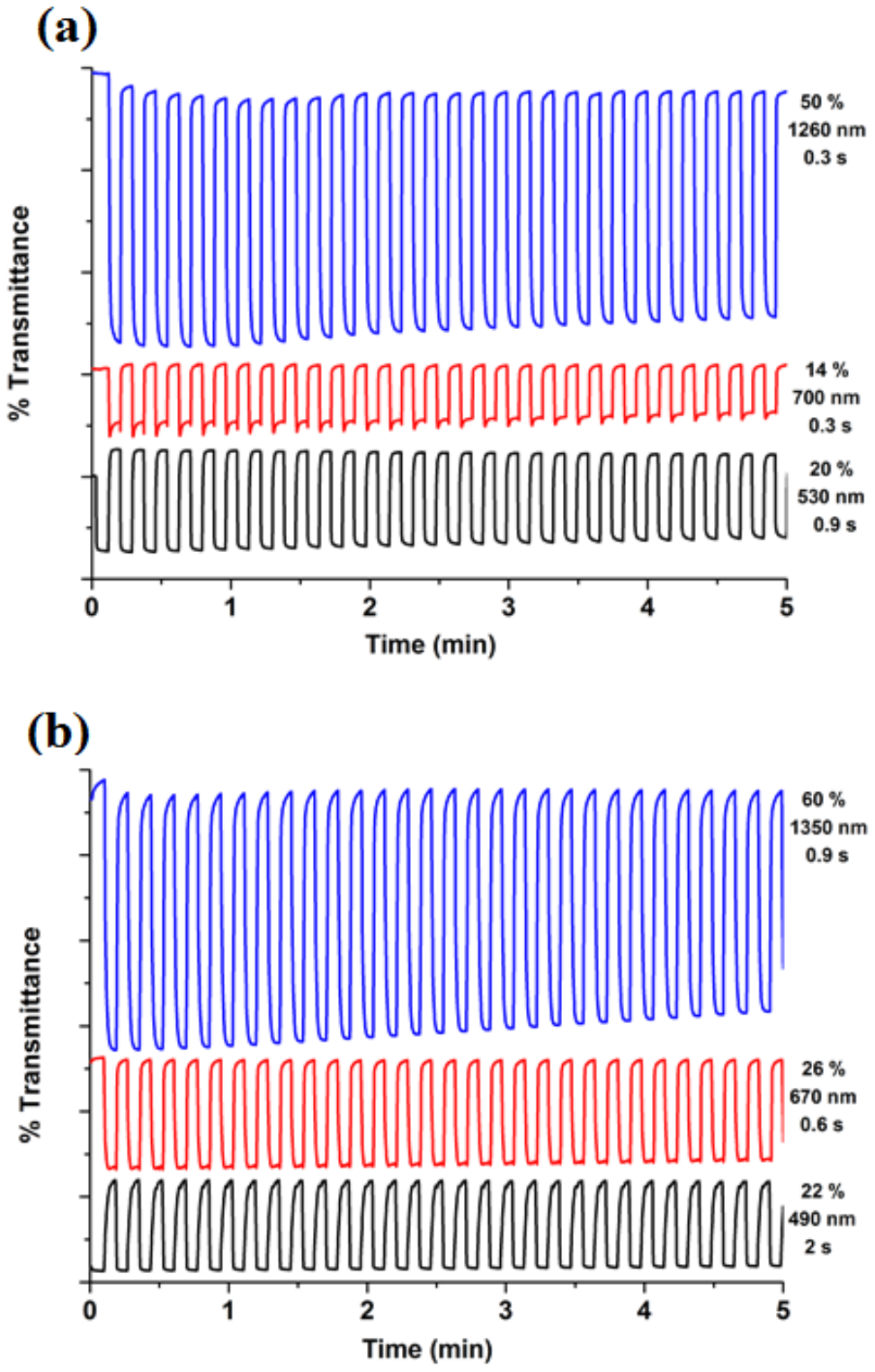

Figure 3.5 Percent transmittance change in **P1** (a) and **P2** (b) in 0.1 M $TBAFP_6$/ACN solution at their maximum wavelengths.

3.5 PhotovoltaicProperties

Preliminary photovoltaic studies of polymers were carried out in the following device structure: ITO/polyethylenedioxythiophene: polystyrenesulfonate (PEDOT:PSS)/active layer/ lithium fluoride (LiF)/aluminum (Al) under AM 1.5 G illumination (100 mW/cm^2). The corresponding device parameters are summarized in **Table 3.3**. Current density–voltage (*J*–V) curves of the OSCs are shown in **Figure 3.6**. The weight ratio of the polymer and [6,6]-phenyl C61 butyric acid methyl ester (PC61BM) was chosen as 1:1 and active layer was spin coated on PEDOT-PSS-coated ITO. Furthermore, LiF and Al were thermally evaporated onto the active layer. The reason for evaporation of LiF between active layer and the cathode is to block the created excitons and to effectuate a dipole at the interface that leads to an increase in charge collection due to the lessened energy barrier at active layer and cathode [51-53].Solvent type affects the phase separation and molecular self-organization since because drying time during film formation influence the film morphology and device performance [54]. Therefore, different solvents were chosen for both polymers. Furthermore, the thickness of the active layer was controlled by changing the rate of the spin coating process. Chloroform was used as the solvent for **P1** (3%, 1:1 weight ratio PCBM:**P1**). It is noteworthy to state that an increase in the Jsc was observed for different thicknesses and the highest value was with a spincoating rate of 2000 rpm resulted in thickness of 90 nm. **P1** showed higher J_{sc} and V_{oc} with a decrease in the thickness of the active layer. Chloroform and chloroform–chlorobenzene mixtures were used as solvents for **P2** (2%, 1:1 weight ratioPCBM:**P2**) to investigate the effect of the solvent. The film quality of **P2** was poor when chloroform was used as the solvent. J_{sc} was enhanced from 0.26 to 1.57 mA/cm^2 and thus PCE was improved from 0.01 to 0.21% by simply switching the solvent from chloroform to chloroform–chlorobenzene; the highest value was observed with a spin coating rate of 1500rpm resulted in a thickness of 80 nm.

TABLE 3.3 Photovoltaic Properties of the Solar Cell Based on **P1** and **P2** with Different Solvents Under the AM 1.5G Illumination

Polymer	Solvent	D/A Ratio	Jsc (mA/cm2)	Voc (V)	FF	PCE (%)
P1	Chloroform	1:1	0.83	0.49	34.2	0.14
P2	Chloroform	1:1	0.26	0.36	25.3	0.01
P2	Chloroform-Chlorobenzene(1:1)	1:1	1.57	0.35	38.2	0.21

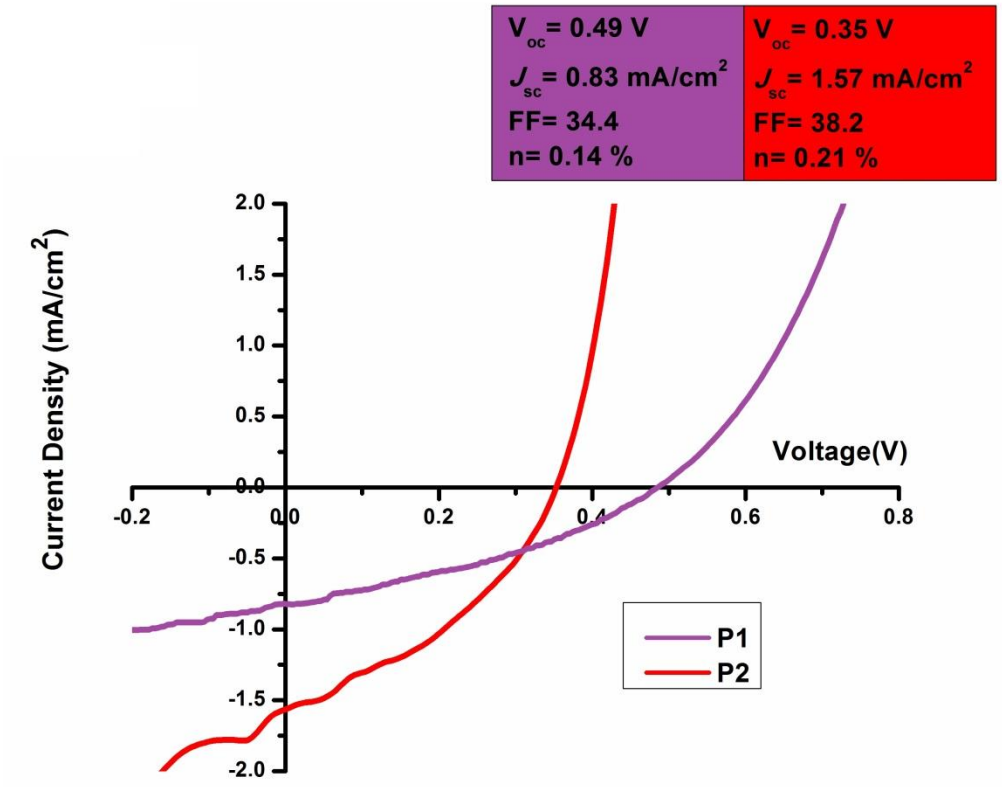

Figure 3.6 Current density versus voltage curves of **P1** or **P2**:PCBM with 1:1 weight ratio under AM 1.5 G illumination (100 mW/cm^2).

The best performance for **P1** device demonstrated a V_{oc} of 0.49 V, a J_{sc} of 0.83 mA/cm^2, a fill factor (FF) of 34.4%, and a PCE of 0.14%. OSC based on **P2** showed a V_{oc} of 0.35 V, a J_{sc} of 1.57 mA/cm^2, a FF of 38.2%, and a PCE of 0.21%. Although both polymers have approximately same HOMO energy level, calculated V_{oc} for **P1** was 0.49 V, which is 0.14 V higher than (0.35 V) OSC based on **P2**. The same trend was also observed with J_{sc}, there is a small difference in band gaps of **P1** (1.85eV) and **P2** (1.60 eV), the observed J_{sc} for **P1** was 0.83 mA/cm2 while for **P2** were 1.57 mA/cm^2. These differences can be attributed to a thickness of the active layer, choice of solvent, and morphology of the active layer.

Incident photon to current efficiencies (IPCE) that provide information about the number of photons that contribute charge separation were compatible with their power conversion efficiencies (IPCE). The average values are found 12% and 13% for **P1** and **P2**, respectively (**Figure 3.7**).

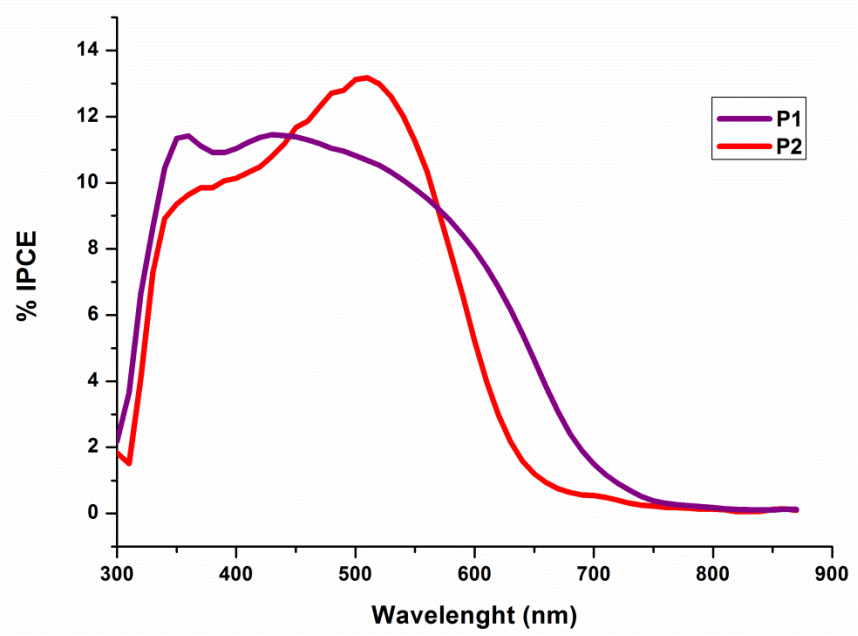

Figure 3.7 IPCEs of the corresponding devices.

Through the convenient band gaps and appropriate HOMO and LUMO energy levels and also wide range absorption of solar spectrum, preliminary studies proved that these parameters cannot be enough to achieve a high performance solar cell. There are many different factors that affect the PCE of photovoltaic devices. Morphology is one of the important factors among others. Thickness of the active layer and its surface roughness is directly related with exciton diffusion. The performance of solar cell can be changed by post-treatments like solvent annealing, thermal annealing, and the usage of the additives. Therefore, morphology and optimization studies of the polymers will be performed in further studies.

CHAPTER 4

CONCLUSION

In this work, poly(4-(dithieno[3,2-b:2,30-d]thiophen-2-yl)-2-(2-octyldodecyl)-2H-benzo[d][1,2,3]triazole) **(P1)** and Poly(4-(5-(dithieno[3,2-b:20,30-d]thiophen-2-yl)thiophen-2-yl)-2-(2-octyldodecyl)-7-(thiophen-2-yl)-2H-benzo[d][1,2,3]triazole) **(P2)** two new DA type copolymers were synthesized. Solubility problems of polymers were meliorated by substituting 2-octyl dodecyl unit on the 2-position of the BTz. Dithienothiophene unit was incorporated BTz and one of BTz derivative to adjust the HOMO and LUMO levels of newly synthesized polymers. Dithienothiophene unit was selected for its superior properties and remarks can be seen in the electrochemical studies. Electrochemical studies represented that **P1** and **P2** had high optical contrast in NIR region and fast switching times. Reported study [55] indicated that incorporation DTT into the structure leads to fast switching times compared with BTz-based polymers and optical transmittance in the near-infrared (NIR) region, which is actually <1s. The reason behind fast switching time was attributed to enhancement of the stability of the quinoid form of the polymer chain. Furthermore, both polymers showed multichromism and ambipolar properties and **P1** exhibited unique full visible absorption with black color at one of the oxidized states. Moreover, electrochemical and optical studies of polymers indicated that they are applicable to the solar cell applications due to a proper alignment of HOMO and LUMO energy levels, suitable band gap and wide range absorption of visible spectrum. GPC, TGA and DSC analysis were done. Although undesired results were obtained from **P2**, low M_n value and sharp peaks on NMR spectrometry, two polymers were intended to be used in OSC. The effect of solvents and thickness of the active layer were investigated. Solvent effect was easily observed in this work and efficiency of devices produced with **P2** was increased from 0.01% to 0.21%. This remarkable change could be attributed to high film quality and successful phase separation throughout the active layer. Preliminary photovoltaic studies of the polymers were represented for **P1** and **P2** as 0.14 % and 0.21 % respectively in this work.

REFERENCES

[1] M. A. Green, K. Emery, D. L. King, Y. Hishikawa, and W. Warta, Prog. Photovoltaics**14**, 455 (2006).

[2]http://optics.org/news/4/1/36, retrieved 27.08.2013.

[3] (S. Barth and H. Baessler,Phys.Rev.Lett. 79, 4445-4448 (1997).

[4] P. G. D. Costa and E. M. Conwell, Am.Phys.Soc.-Rap.Comm.48, 1993-1997 (1993).

[5] R. N. Marks, J. J. M. Halls, D. D. C. Bradley, R. H. Friend and A. B. Holmes, J. Phys.: Cond. Mat. 6, 1379-1394 (1994).

[6]Y. Li andY. Zou, Adv. Mat.,20,2952–2958 (2008).

[7] C. Winder, N. S. Sariciftci, J. Mater. Chem., 14, 1077-1086 (2004).

[8] H. A. M. van Mullekom, J. A. J. M. Vekemans, E. E. Havinga and E. W. Meijer, Material Science and Eng. 32, 1-40 (2001).

[9] E. E. Havinga, w. ten Hoeve and H. Wynberg, Synthetic Metals, 55, 299-306 (1993).

[10] U. Salzner, J. Phys. Chem. B, 106, 9214-9220 (2002).

[11] U. Salzner, Synthetic Metals, 119, 215-216 (2001).

[12] U. Salzner, J. Phys. Chem. B, 106, 9214-9220 (2002).

[13] J. Roncali, Chem. Rev., 97, 173-205 (1997).):

[14]. G.A. Chamberlain, Organic Solar Cells: A Review, Solar Cells 8, 47 (1983).

[15] D. Wöhrle and D. Meissner, Organic Solar Cells, Adv. Mater. 3, 129 (1991).

[16] . C.J. Brabec, N.S. Sariciftci, and J.C. Hummelen, Plastic Solar Cells, Adv. Funct. Mater.11, 15 (2001).

[17] J.J.M. Halls and R.H. Friend, in Clean Electricity from Photovoltaics, edited by M. D. Archer and R. Hill (Imperial College Press, London, 2001).

[18] J. Nelson, Organic photovoltaic films, Curr. Opin.Solid State Mater.Sci. 6, 87 (2002).

[19] J.-M. Nunzi, Organic photovoltaic materials and devices, C. R. Physique 3, 523 (2002).

[20] Organic Photovoltaics: Concepts and Realization; Vol. 60, edited by C.J. Brabec, V. Dyakonov, J. Parisi, and N.S. Sariciftci (Springer, Berlin, 2003).

[21] P. Peumans, A. Yakimov, and S.R. Forrest, Small molecular weight organic thin-film photodetectors and solar cells, J. Appl. Phys. 93, 3693 (2003).

[22]B. Maennig, J. Drechsel, D. Gebeyehu, P. Simon, F. Kozlowski, A. Werner, F. Li, S. Grundmann, S. Sonntag, M. Koch, K. Leo, M. Pfeiffer, H. Hoppe, D. Meissner, S. Sariciftci, I. Riedel, V. Dyakonov, and J. Parisi, Organic p-i-n solar cells, Appl. Phys. A 79, 1 (2004).

[23] C.D. Dimitrakopoulos and D.J. Mascaro, Organic thin-film transistors: A review of recent advances, IBM J. Res. Dev. 45, 11 (2001).

[24] L.A.A. Pettersson, L. S. Roman, and O. Inganas, J. Appl. Phys., 86 (1), 487-496 (1999).

[25] N. F. Mott,Proc.Cambr.Phil. Soc. 34, 568-572 (1938)

[26] W. Schottky, Naturwiss. 26, 843 (1938).

[27] J. J. M. Halls, PhD thesis, Cambridge (1997).

[28] M. Granstrom, K. Petritsch, A. C. Arias, A. Lux, M. R. Andersson and R. H. Friend, Nature 395, 257-260 (1998).

[29] W. Shockley and H. J. Queisser,J.Appl.Phys. 32, 510 (1961).

[30] M.A. Green, University of New South Wales, Kensington, (1992).

[31] R. Gottschalg, T.R. Betts, D.G. Infield, and M.J. Kearney, Solar Energy Materials and Solar Cells, 85,415-428, (2005).

[32] J. R. Platt, The Journal of Chemical Physics, 34, 862-863, (1961).

[33] S.K. Deb and J.A. Chopoorian, J. Appl. Phys. 37, 4818, (1968).

[34]H. Shirakawa, E. J. Louis, A. G. MacDiarmid, C. K. Chiang, and A. J. Heeger, J.

Chem. Soc., Chem. Commun. 578, (1977).

[35]G. Yu and A.J. Heeger, J. Appl. Phys. 78, 4510 (1995).

[36]B. W. Rossiter and J. F. Hamilton, “Physical Method of Chemistry, ElectrochemicalMethods”, Vol II, John Wiley and Sons.Inc. New York, 1986

[37] (a) Z. He, C. Zhong, X. Huang, W.-Y. Wong, H. Wu, L. Chen,S. Su, and Y. Cao, Adv. Mater., 23, 4636–4643(2011); (b) Z. He, C.Zhong, S. Su, M. Xu, H. Wu, and Y. Cao, Nat. Photonics, 6, 591–595 (2012).

[38] (a) A. Balan, G. Gunbas, A. Durmus, and L. Toppare, Chem. Mater., 20, 7510–7513 (2008); (b) A. Balan, D. Baran, G. Gunbas,A. Durmus, F. Ozyurt, and L. Toppare, Chem. Commun.,6768–6770 (2009); (c) E. Kaya, D. H. Apaydın, D. E. Yıldız, L. Toppare, and A. Cirpan, Sol. Energ. Mat. Sol. C, 99, 321–326 (2012); (d) D.Baran, A.

Balan, S. Celebi, B. M. Esteban, H. Neugebauer, N. S.Sariciftci, and L. Toppare, Chem. Mater., 22, 2978–2987 (2010); (e) Z.Zhang, B. Peng, B. Liu, C. Pan, Y. Li, Y. He, K. Zhou, and Y. Zou,Polym.Chem., 1, 1441–1447 (2010).

[39]S. C. Price, A. C. Stuart, L. Yang, H. Zhou, and W.You, J. Am.Chem. Soc., 133, 4625–4631 (2011).

[40] Y.-X. Xu, C.-C.Chueh, H.-L.Yip, F.-Z.Ding, Y.-X.Li, C.-Z. Li,X. Li, W.-C. Chen, and A. K.-Y. Jen, Adv. Mater., 24,6356–6361 (2012).

[41](a) H.-P. Fang, I.-H.Chiang, C.-W.Chu, C.-C.Yang, and H.-C. Lin,Thin Solid Films, 519, 5212–5218 (2011); (b) J. Li, H.-S.Tan, Z.-K.Chen, W.-P.Goh, H.-K.Wong, K.-H.Ong, W. Liu, C. M. Li, and B. S.Ong, Macromolecules, 44, 690–693 (2011); (c) S. Millefiorini, E.Kozma, M. Catellani, and S. Luzzati, Thin Solid Films, 516,7205–7208 (2008).

[42]S. S. Zhu, and T. M. Swager, J. Am. Chem. Soc., 119,12568–12577 (1997).

[43]X. Zhan, Z. Tan, B. Domercq, Z. An, X. Zhang, S. Barlow, Y.Li, D. Zhu, B. Kippelen, and S. R. Marder, J. Am. Chem. Soc.,129, 7246–7247 (2007).

[44] A. Tanimoto, and T. Yamamoto, Adv. Synth. Catal., 346,1818–1823 (2004).

[45]G. Hızalan, A. Balan, D. Baran, and L. Toppare, J. Mater. Chem., 21, 1804–1809 (2011).

[46]J. Min, Z.-G. Zhang, S. Zhang, M. Zhang, and J. Zhang, Y. Li,Macromolecules, 44, 7632–7638 (2011).

[47]P. M. Beaujuge, S. Ellinger, and J. R. Reynolds, Nat. Mater., 7, 795–799 (2008).

[48]N. Akbasoglu, A. Balan, D. Baran, A. Cirpan, and L. Toppare, J.Polym. Sci. Part A: Polym. Chem., 48, 5603–5610 (2012).

[49]K. Aydemir, S. Tarkuc, A. Durmus, G. E. Gunbas, and L. Toppare,Polymer, 49, 2029–2032 (2008).

[50]A. A. Argun, P.-H.Aubert, B. C. Thompson, I. Schwendeman,C. L. Gaupp, J. Hwang, N. J. Pinto, D. B. Tanner, A. G.MacDiarmid, and J. R. Reynolds, Chem. Mater., 16, 4401–4412 (2004).

[51]C. J. Brabec, S. E. Shaheen, C. Winder, N. S. Sariciftci, and P.Denk, Appl. Phys. Lett., 80, 1288–1290 (2002).

[52]S. K. M. Jönsson, E. Carlegrim, F. Zhang, W. R. Salaneck, and M. Fahlman, Jpn. J. Appl. Phys., 44, 3695–3701 (2005).

[53]H. J. Park, Y. Lee, J. W.Jo, and W. H.Jo, Polym. Chem., 3,2928–2932 (2012).

[54]L.-M. Chen, Z. Hong, G. Li, and Y. Yang, Adv. Mater., 21,1434–1449 (2009).

[55] S. C. Cevher, N. A. Unlu, A. C. Ozelcaglayan, D. H. Apaydin, Y. A. Udum, L. Toppare, A. Cirpan, J. Polym. Sci. Part A: Polym. Chem., 51, 1933-1941 (2013).

APPENDIX A

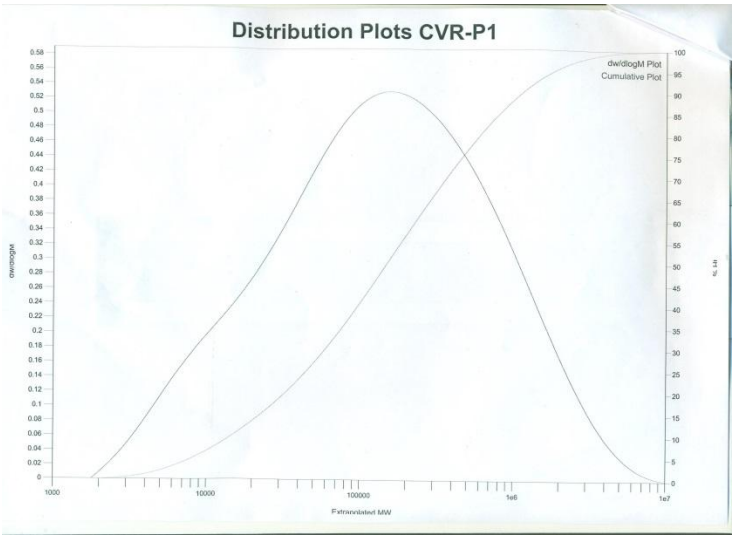

Figure A.1 GPC result of P1

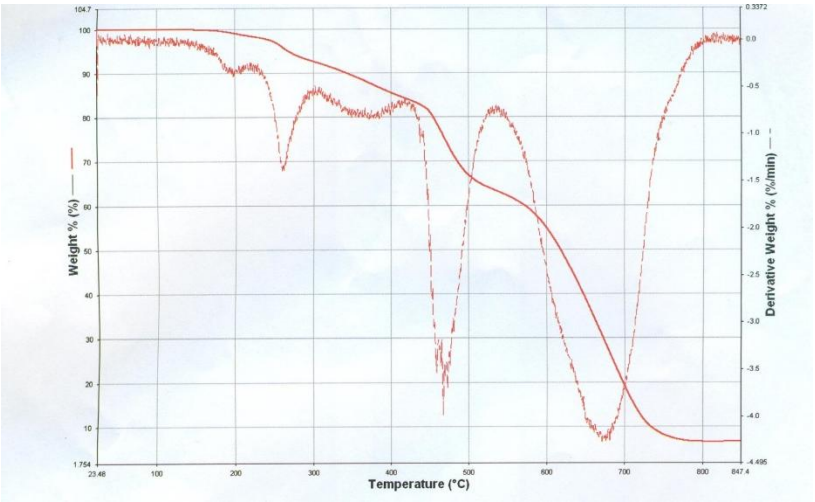

Figure A.2 TGA result of P1

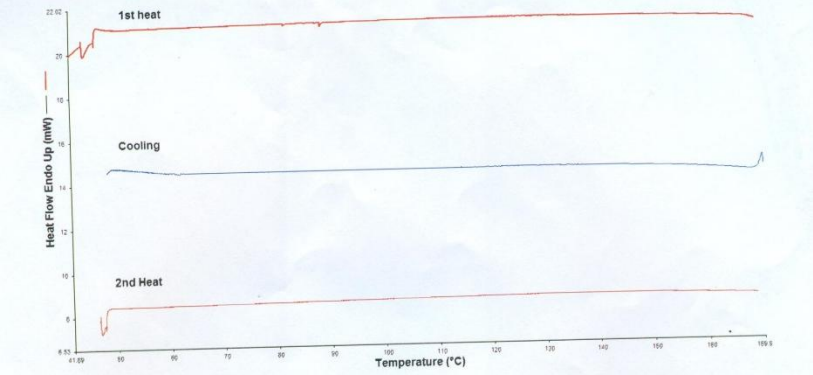

Figure A3 DSC result of P1

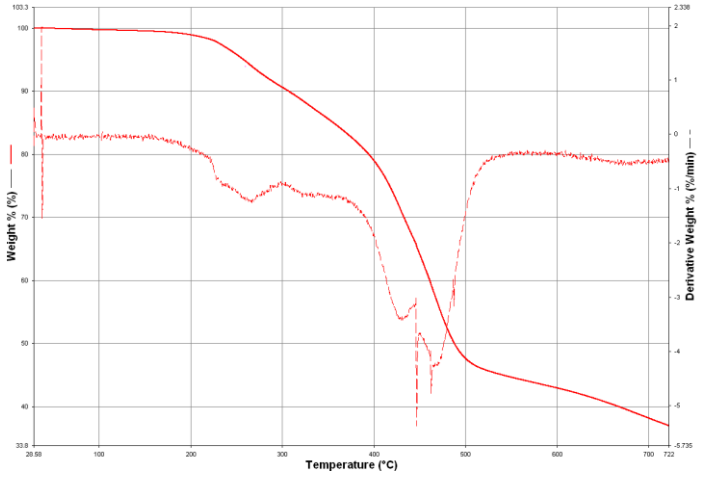

Figure A.4 TGA result of P2

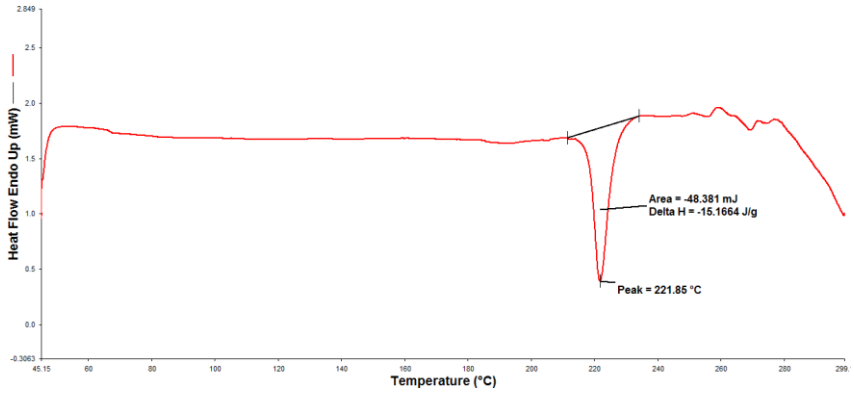

Figure A.5 DCS result of P2

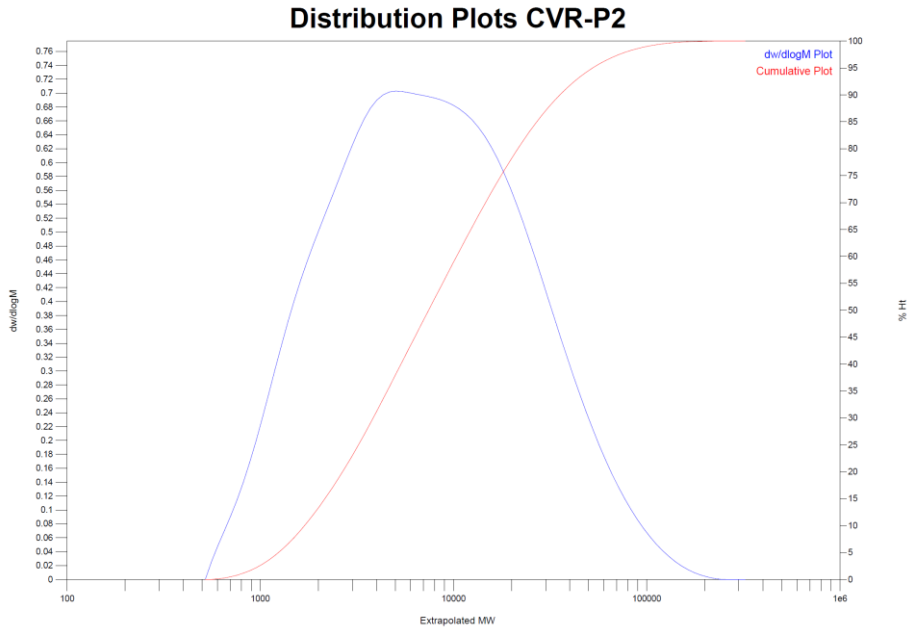

Figure A.6 GPC result of P2